Chapter 3
Radio Resource Management for Device-to-Device Communications in Long Term Evolution Networks

Carlos F. M. Silva, José Mairton B. Silva Jr. and Tarcisio F. Maciel

3.1 Introduction

Direct communication between wireless devices—the so-called Device-to-Device (D2D) communication—has gradually gained attention in the scientific community and industry over the last decade, and became a quite extensive research field. In this section, we intend to introduce the concept of D2D communications in wireless networks in general and further guide the reader toward D2D communications as underlaying the next generation of cellular networks and the related Radio Resource Management (RRM) problems in that context. As such, the following paragraphs, when not clearly stated otherwise, are targeted for a Long Term Evolution (LTE) or LTE-Advanced compliant networks.

Before going further, let us first introduce some names. In the next list, we shortly give an insight about the meaning of important terms that are commonly used in the remaining paragraphs. This is not an exhaustive definition as they are better defined when required.

- **Evolved Node B (eNB)** is the term coined by 3rd Generation Partnership Project (3GPP) to refer a LTE Base Station (BS).
- **User Equipment (UE)** is the terminal or user's device, also general referred as network node.

C. F. M. Silva (✉) · J. M. B. Silva Jr. · T. F. Maciel
Wireless Telecommunications Research Group (GTEL), Federal University of Ceará,
Caixa Postal 6005, Fortaleza 60440-900, Brazil
e-mail: cfms@gtel.ufc.br

J. M. B. Silva Jr.
e-mail: mairton@gtel.ufc.br

T. F. Maciel
e-mail: maciel@gtel.ufc.br

Francisco Rodrigo Porto Cavalcanti (ed.), *Resource Allocation and MIMO for 4G and Beyond*, DOI: 10.1007/978-1-4614-8057-0_3,

- **Neighbor** of the reference node is a node in the surroundings of the latter in a such way that the former's power (plus interference and noise) is received above the predefined threshold.
- **$\mathbf{D2D_{Tx}}$** is the transmitter device in the D2D communication.
- **$\mathbf{D2D_{Rx}}$** is the receiver device in the D2D communication.
- **D2D pair** is the pair formed by $D2D_{Tx}$ and $D2D_{Rx}$.
- **Cellular pair** is the pair formed by a transmitter and receiver in cellular mode. The transmitter/receiver can be a regular UE or an eNB.

The remaining of the section is organized as follows: in Sect. 3.1.1 the principal concepts related with D2D communications are introduced; in Sect. 3.1.2 the neighbor discovery process is explained and its main algorithms are identified in a state-of-art review; and in Sect. 3.1.3 a literature review highlights the main Radio Resource Allocation (RRA) mechanisms for D2D communications.

3.1.1 Concept of D2D Communications

D2D communication[1] is a type of direct wireless communication between two or more nodes similar to the direct mode in professional mobile radio systems (colloquially, walkie talkies).[2] D2D communications can be deployed in ad hoc wireless networks for the unlicensed spectrum use, like Wireless Local Area Network (WLAN) networks, or in cellular networks for the licensed use, such as LTE and LTE-Advanced.

The main principle that underlays D2D communication is to exploit the nodes' proximity that may allow very high data rates, low delays, and power consumption [22]. For the D2D communication between nodes in close proximity when considering a cellular network, the network operator does not need to be involved in the actual data transport, except (eventually) for the signaling of session setup, charging, and policy enforcement; which alleviates the core network from the data transport.

The other benefits of D2D communication are the reuse gain and hop gain. The reuse gain implies that radio resources may simultaneously be used by cellular and D2D links, tightening the reuse factor (even for reuse-1 systems). The hop gain refers to the use of a single link in D2D mode rather than using uplink and downlink bands (Frequency Division Duplex (FDD)) or different time slots (Time Divison Duplex (TDD)) like in cellular mode [25]. Additionally, at cell boundaries, D2D links may be also used to extend the cell coverage area.

Despite its advantages, the existence of D2D communication pose a new challenge: nodes and network must cope with new interference situations. For example, in cellular networks using Orthogonal Frequency-Division Multiplexing (OFDM) technology, the D2D links may reuse some of the allocated Physical Resource Blocks

[1] Sometimes also referred as Peer-to-Peer (P2P) communication.

[2] See the Terrestrial Trunked Radio Access (TETRA) standard [23].

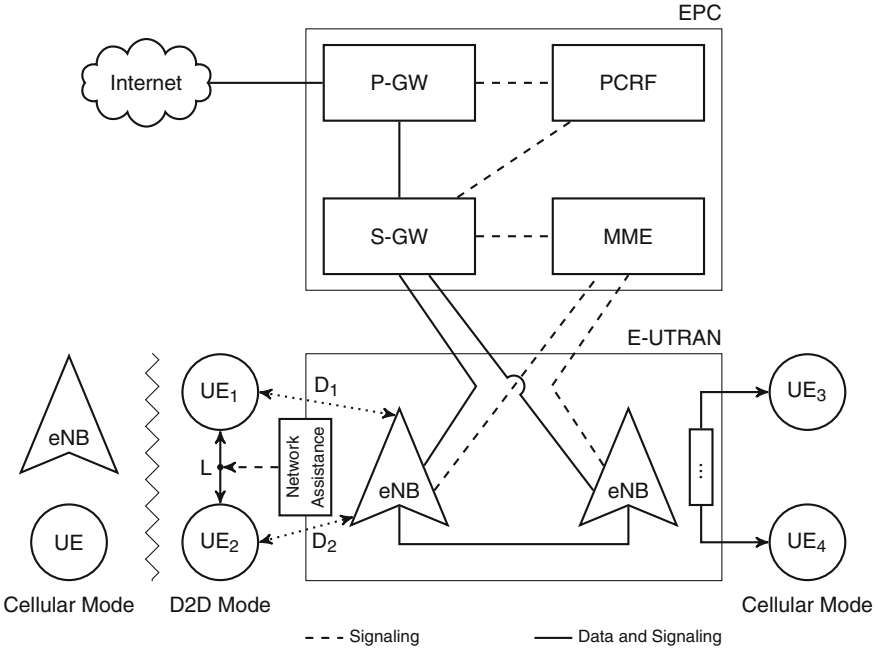

Fig. 3.1 D2D communication underlaying a LTE-like network

(PRBs); and, in such case, the intracell (or co-channel) interference is no longer negligible because the orthogonality between links is lost. Moreover, the undesirable proximity of D2D and cellular transmitters/receiver may bring new types of intercell interference. Nevertheless, the new types of interference also depend on the duplexing scheme, spectrum bands, and resources allocation algorithms.

In Fig. 3.1 a simplified LTE network with a D2D communication is presented. The UE_3 is in cellular mode, i.e., if it tries to communicate with UE_4, it first needs to send a session request to the eNB. After the permission is granted, the eNB mediates the whole session and forwards the traffic to the respective node. UE_1 and UE_2 are in D2D mode; D_1 and D_2 denotes the distance between D2D nodes and eNB, while L denotes D2D link distance, where usually $L \ll \{D_1, D_2\}$.

When UE_1 attempts to communicate with UE_2 (or vice-versa), interference may happen in the uplink direction toward the eNB or in surrounding nodes that are in cellular mode (intracell interference). If the D2D communication happens at cell-edge, the interference may be caused in the eNBs or nodes in the vicinity cells (intercell interference). The proposed solutions to deal with this problem include: spatial diversity [31], mode selection [21], power control [53], or advanced coding schemes [19].

Hence, the key functions for D2D communications comprise: neighbor discovery, physical layer and Media Access Control (MAC) sublayer procedures, like syn-

chronization and reference signal design, RRM functions such as mode selection, scheduling, power control, and interference coordination [25].

3.1.2 Neighbor Discovery for D2D Communications

Neighbor discovery, as described in [11], is the determination of all nodes in the network with which a given node may directly communicate with, i.e., establish a D2D communication. Knowledge of neighbors is essential for all routing protocols, medium access control protocols, and several other topology control algorithms. Ideally, nodes should discover their neighbors as quickly as possible, which enables them to save energy in their discovery phase. Also, a speedy discovery allows other protocols (such as routing protocols) to quickly start their execution. In addition, neighbor discovery may also be the solution for partner selection in cooperative wireless networks. The number of neighbors is typically orders of magnitude smaller than the size of all network interface addresses, so neighbor discovery is by nature compressed sensing (or sparse discovery) [54].

Immediately after the ad hoc network deployment, a node has no knowledge about the other nodes in its transmission range and needs to discover its neighbors. Therefore, the neighbor discovery process is one of the first steps in the configuration of large wireless networks [46]. The problem becomes crucial in self-organizing networks without preexisting infrastructure [54].

The neighbor discovery shall not significantly decrease the operation time of UEs to be accepted by users and be adaptive to very sparse environments, with few nodes, to crowded places. In a crowded place, the discovery process becomes challenging as well as keeping the energy consumption low. In sparse environments it may happen that there is no neighbors and the scanning process shall not completely drain the UE's battery [20]. Furthermore, energy efficiency in maintaining the network and guaranteeing a low duty cycle [51] are also desirable.

The final step in the D2D link establishment procedure is to trigger a beacon between the D2D server and client (or $D2D_{Tx}$ and $D2D_{Rx}$) to evaluate the actual quality of the channel and build the required routing tables. In LTE-like networks, the D2D link quality is reported to the eNB and serves as the basic input to mode selection [21].

3.1.2.1 Disambiguation

One may confuse the neighbor discovery (sometimes also referred in literature as peer discovery) in the context of D2D communications with BitTorrent services[3] and their peer discovery mechanism. First, there is a clear difference in the concept,

[3] BitTorrent is a P2P file sharing protocol used for distributing large amounts of data over the Internet [14].

studied problems, and proposed solutions; second, the D2D communication focus the physical and link layers, namely MAC sublayer; while BitTorrent is a service and, therefore, considered in upper layers (network, transport, and application).

Moreover, D2D communications are being proposed for ad hoc wireless networks, and also for the cellular domain as an underlay (secondary) network of the primary one [22]. Hence, the nodes participating in D2D communications form a network that is capable of exchanging data: transfer files, voice conversation, audio and video streaming, or other kind of services.

The D2D-related mechanisms are somehow similar to the ones that do exist in Bluetooth technology[4]—peer discovery and device paring—where the so-called *inquiry process* allows a potential master node to identify other nodes in range that wish to participate in a piconet, whereas the *paging process* allows the master node to establish links toward the desired slave nodes [25].

3.1.2.2 Algorithms Classification

According to [46] the neighbor discovery algorithms can be classified in two main categories: randomized or deterministic. However, many other divisions may also apply, depending on the type of, e.g., technology, network organization, focused layers, antennas, protocols, or signaling methods. A good discussion on neighbor discovery algorithms (namely for ad hoc networks) and their classification can be found in [10, 55].

Considering the type of network and the knowledge of its structure, the neighbor discovery algorithms may be used in deterministic or random networks. In a deterministic network the structure is mostly static and well-known, therefore reorganizations are infrequent. On the other hand, for random networks, the neighbor discovery algorithms must cope with uncertainty and common reorganizations due to, e.g., entrance/exit of nodes and their movement, and thus parameters may drastically change between sessions [22, 24, 45]. For random networks, the list of neighbors and routing tables shall at least be updated before the establishment of each data link, while for deterministic networks, the bootstrap configuration (this is, when nodes are turned on) may be sufficient to keep lists updated.

Neighbor discovery protocols are sometimes generally classified as one-way neighbor discovery or handshake-based neighbor discovery [9]; they can also be classified as power detection or protocol-oriented, respectively. Power detection neighbor discovery requires that each node periodically sends out advertising packets (in random or defined directions) to announce its presence, and neighbors are discovered by receiving their advertising packets [20]. For protocol-oriented neighbor discovery, a node needs to provide active response to the sender after receiving an advertising packet from an unknown neighbor. Protocol-oriented neighbor discovery is usually implemented at MAC sublayer, while power detection neighbor discovery is in physical layer. Relying only on power detection, i.e., carrier sensing at physical layer, may led to undetected neighbors and the *hidden node problem*.

[4] See http://bluetooth.org.

Actually, the *hidden node problem* is one of the main sources of packet collision in wireless networks: when two or more nodes attempt to transmit a packet across the network at the same time, a packet collision occurs. Although, if a collision occurs and no recover is possible, the detection of neighbors can be compromised. Collisions may be avoided by the use of wide-spaced channels, carrier sensing mechanism (which are implemented at MAC sublayer), or at modulation level, like using OFDM-based schemes [35, 55]. Moreover, synchronous (or slotted) detection may also be implemented to mitigate collisions and, therefore, all nodes transmit following a common reference frame, which is allowed with the distribution of a local clock [10]. In asynchronous detection, there is no cooperation between nodes. Hence, their transmission slots are misaligned which conduct to detections up two times slower than synchronous counterpart [40, 46].

Other common division to evaluate the probability and required time to detect all neighbors, is the distinction between randomized and deterministic neighbor discovery [46]. In randomized neighbor discovery, each node transmits at randomly chosen times and neighbors are detected with high probability within a predefined timeout. In a deterministic neighbor discovery, each node transmits according to a predetermined schedule which allows the detection of all neighbors during the timeout. In deterministic neighbor discovery, the transmission may occur, e.g., like in the well-known *token ring protocol* that exists for wired networks; where token-possession grants the possessor permission to transmit on the medium, i.e., when a node transmits, the other nodes listen, thus avoiding collision problems. In randomized neighbor discovery, collisions are likely to occur. In Refs. [46, 51] the detection of neighbors is reduced to *coupon collector's problem*, where the time to detect all neighbors is lower and upper bounded with closed form expressions.

Regarding the type and number of antennas, two division can be considered: the use of omnidirectional or directional antennas, and Single-Input-Single-Output (SISO) or Multiple-Input-Multiple-Output (MIMO) schemes. Many neighbor discover protocols have been proposed that use directional antennas. Directional antennas concentrate their beams according to specific directions, which enables selectivity in the reception (along with the increase of Signal-to-Interference-plus-Noise Ratio (SINR)) and for a given transmission power, the communication range is greatly extended [45]. However, the *hidden node problem* [42] and *deafness* [27] due to misalignment in transmitter and receiver's antennas are common problems. As such, protocol design using directional antennas is a challenging problem, while neighbor discovery is seen as relatively simpler problem when omnidirectional antennas are used because a simple broadcast can reach all nodes within the transmission range [24].

For the spatial diversity, conventional MIMO schemes require that both the transmitter and receiver must be equipped with multiple antenna arrays. In practice, however, many nodes may not be able to support multiple antennas due to size, cost, and/or hardware limitations. For D2D communications an alternative approach is to use cooperative MIMO: there is group multiple nodes into virtual antenna arrays to emulate MIMO communications [48]. For example, when a target node temporarily suffers from bad channel conditions or requires relatively high rate service,

its neighboring nodes can help to provide multihop coverage or increase the data rate by relaying information to the target node, or even detect nodes that were inaccessible in other way. Typical neighbor discovery algorithms use SISO, thus they can only provide one-hop information.

Finally, neighbor discovery algorithms can also be divided according to the type of network for which they were projected. In the self-sufficient (or unsupervised) neighbor discovery algorithms, the nodes rely only on themselves to detect neighbors. There is no central coordinator node neither a central database of yet discovered nodes. Typically, self-sufficient algorithms are implemented in wireless ad hoc networks. On the other hand, the network-assisted (or supervised) neighbor discovery is likely to be implemented in typical cellular networks, where the access network (and core network) cooperate with UEs to detect D2D candidates [22]. In network-assisted neighbor discovery, the identification of D2D candidates can be done using *a-priori* or *a-posteriori* schemes [25]. The *a-priori* scheme is used if UE or network detects D2D candidates just before commencing the communication data session between UEs in cellular mode; while *a-posteriori* scheme is employed if D2D candidates are only detected during the ongoing cellular communication sessions.

3.1.3 RRA for D2D Communications

The use of RRA techniques such as user grouping, adaptive scheduling, mode selection, and power control can improve the benefits of D2D communications to cellular systems and, for this purpose, it has been a topic of intense research in the last few years [22, 25]. In Fig. 3.2 those procedures are presented in a (possible simulation) chain before the link establishment. Note that we named the RRM as the whole

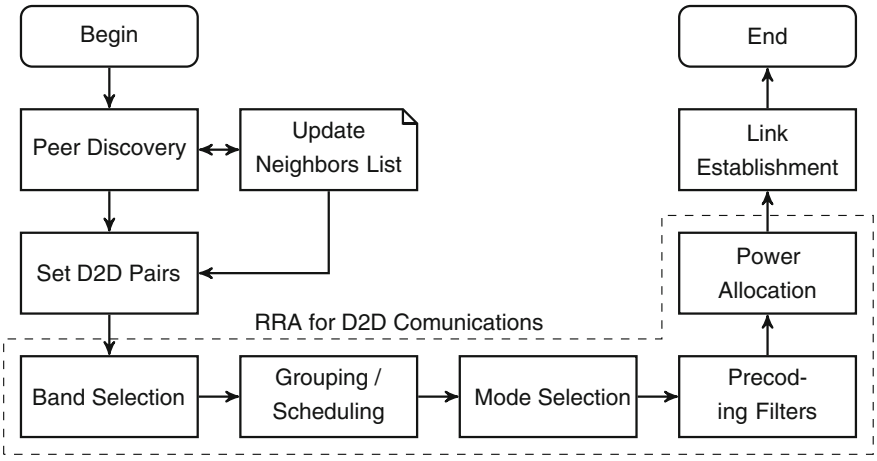

Fig. 3.2 RRM procedures for D2D communications and link establishment

chain and the techniques that really deal with resource allocation as RRA for D2D communications.

Scheduling procedure is responsible for defining which flows are scheduled and determining their required data rates at a specified time, while the resource assignment feature defines which resources will be assigned to the selected flows. Key aspects for designing a mode selection and D2D resource allocation in network-assisted D2D communication, that both addresses the intracell interference and time scale for channel quality estimation can be found in [25].

Furthermore, the resource allocation between cellular and D2D users have also been addressed in Refs. [32, 47, 56]. In Ref. [56], a greedy heuristic algorithm considering channel gain information appropriately selects the shared radio resources among D2D and cellular users. In Ref. [32], the authors exploit the multiuser diversity inherent in cellular systems to improve the network performance. And in Ref. [47] the D2D users can reuse the resources of more than one cellular user in a system where full Channel State Information (CSI) is assumed, improving the whole system spectral efficiency.

Concerning the mode selection, in Ref. [22] by allowing D2D communication to underlay the cellular network, the overall throughput in the network may increase up to 65 % when compared to the traditional case where all traffic is relayed through the cellular network. Moreover, in Ref. [33] semi-analytical studies have shown that when D2D communications share the same resources as the cellular network, significant gains in sum rate can be achieved compared to the conventional case, namely by the jointly and optimal allocation. Nevertheless, numerical analysis have also shown that communication mode selection algorithms need to be designed with careful to prevent deteriorating of the whole system performance.

In line with the previous, in Ref. [29] by means of getting optimal communication mode for all devices in the system, equations are derived that capture the network information such as link gains, noise levels, and SINRs. According to the results, the main factors affecting the performance gain of D2D communication are the local communication probability and maximum distance between communicating nodes, as well as the communication mode selection algorithm. As such, designing efficient D2D communication mode algorithms with minimal interference to the cellular network is seen as a major requirement.

Additionally, in Ref. [21] the eNB can decide whether the underlaying D2D pair should reuse cellular resources, get dedicated resources or communicate via eNB. It concludes that optimal communication mode selection strategy does not only depend on the quality of the link between D2D terminals and the quality of the link toward the eNB, but also on the interference situation. In a multicell scenario also the interference from other cells will affect the decision. In other words, it largely depends on the position of the D2D receiver ($D2D_{Rx}$) relative to the cellular terminal when reusing uplink resources, and to the eNB when reusing downlink resources.

Power control is a well-known RRM strategy for interference management in multiuser communication systems. In these systems, the performance of a UE depends on its own transmit power as well as on the transmit powers of interfering UEs. Power control usually improves system performance by adjusting transmit

powers of the co-channel UEs so that each of them attains its target Quality of Service (QoS), often expressed as a SINR value. In this way, links with in-excess QoS will have their transmit powers lowered, thus reducing (battery) power consumption as well as interference levels in the system [15, 16, 18, 26, 28, 38, 41, 50].

Power control algorithms for cellular systems have been studied with fixed [16, 26, 41] and variable [15, 18, 28, 38, 50] target SINR values considering scenarios with single- [15, 26, 28, 50] and multiple-antenna transceivers [15, 16, 18, 38, 41]. Several power control algorithms have been proposed in the literature [15, 16, 18, 28, 38, 41] based on the interference function model proposed by Yates in Ref. [50], which shows that power control iterations (in t) of the form $p_k^{(t+1)} = I(p_1^{(t)}, \ldots, p_K^{(t)})$, $\forall k$ always converge to optimum powers $p_k^{\star}$, $\forall k$ whenever the interference function $I(\cdot)$ possesses some special properties. A detailed review of power control based on interference functions is out of the scope of this chapter, but can be found in Ref. [15].

In particular, power control algorithms originally designed for multicell systems can be adapted to scenarios with D2D communications by looking at D2D transmitters as the transmitters of interfering cells. Because D2D communications in a LTE-like system can be seen as an underlay, some works focused on limiting the impact of these communications on the cellular ones [49, 52, 53]. In Ref. [52], the SINR distribution of D2D and cellular users is determined and a simple power control algorithm that limits the impact of D2D communications on the cellular ones is investigated, while in Ref. [53] two power control algorithms are analyzed: a power optimization with greedy sum rate maximization and a power optimization with rate constraints. Similarly, different power control schemes for D2D UEs communicating in the uplink of a LTE system have been studied in Ref. [49]. In these works the authors reached the same conclusions: power control can improve the whole system performance in comparison with a pure cellular system and, with proper scheduling and mode selection algorithms, also minimize the generated interference.

In Ref. [12] the authors studied a joint mode selection, scheduling and power control problem, which aimed to minimize the used sum power. The scenario was composed of two circular cells, one D2D-capable pair and two cellular UE. The authors developed a suboptimal algorithm considering mode selection and scheduling, because the joint problem was Non-deterministic Polynomial-time (NP)-hard and, therefore, the optimum solution might not be useful in practice. The performance metrics were the consumed power and the total spectral efficiency, which were analyzed for different distances of the D2D pair and cellular UEs and for different transmission modes. Results showed that when the D2D communications could reuse the cellular spectrum resources, the overall capacity was increased, mainly when the joint mode selection and power control were used.

In Ref. [34] the authors also studied the joint mode selection and power allocation problem, but aiming to a sum power minimization and capacity maximization. The scenario was composed of one circular cell, one D2D-capable pair and one cellular UE. In order to jointly consider those goals, it was proposed an utility function as power efficiency, defined as the overall system capacity per total power. The authors

also derived an upper and lower bounds to the utility function. Based on the utility function and the bounds, it was proposed an algorithm which performs an exhaustive search in the set of all possible mode sequences and choses the best one. From the results, the proposed algorithm performed close to the delivered upper bound, but had the disadvantage of huge computational effort.

In a scenario with multiple users and a limited number of resources, the choice of which users will be allocated is a key parameter, impacting directly in the data rate of the system. The usage of grouping techniques can improve the total systems' data rate by choosing users which share similar properties, e.g., orthogonality and distance to the eNB, to reuse the same resource, thus reducing the interference.

In Ref. [43], the authors propose a spatial subchannel allocation method that sequentially assigns a spatial subchannel to a certain group of channels so that no interference is generated by the currently added spatial subchannel to any of the previously grouped ones. The interference originated by a certain subchannel on subsequently established subchannels is neutralized by successive encoding following a Zero-Forcing (ZF) criterion. Similarly to Ref. [43], in Ref. [13] it is proposed to admit UEs to the group in order to improve the channel gain after a projection onto the null space of the channels of the already admitted UEs, so that previously admitted UEs do not see any interference from UEs posteriorly admitted to the group.

Generally speaking, in D2D communications as underlaying a multiuser and multicell network, the group can be formed by a D2D pair along with an already scheduled cellular UE based on some grouping metric which measure the compatibility among them. Furthermore, spatial subchannel allocation to create mixed groups of D2D and cellular UEs and its usage with precoding and power allocation techniques are potential techniques to mitigate the interference created by the multiple users inside the group, which will be explored in next sections.

3.2 RRA for D2D Communications Underlaying LTE Networks

As it has been discussed in Sect. 3.1, direct D2D communication in wireless networks has been a desired feature for considerable time due to all its many potential benefits. Despite that, D2D communication as an underlay of cellular networks has only received considerably attention recently; as such, it is considered a relatively novel field, for which getting additional insight on how D2D communication can improve the overall network performance is still required.

In this section, we try to provide some insightful information on the performance of D2D communications underlaying a LTE-like network and, in particular, we consider their interaction with important network RRA features, such as mode selection, resource allocation, power control, and user grouping. For this purpose, we study D2D communications considering relatively simple scenarios capable, however, of showing how this new type of communications can significantly improve the system performance.

3.2.1 System Modeling

Herein we present the layout of cellular system and the adopted modeling for the multiple access among UEs in our scenario, as well as the modeling of propagation effects on the links between the transmit/receive antennas of the network nodes, and it is also briefly described the signal model considered in most performance evaluations of the chapter.

3.2.1.1 Cellular System Layout

We consider a LTE-like system scenario consisting of two circular cells of radius R_c, each having one eNB at its center. In the most basic configuration, one conventional UE and a pair of D2D-capable UEs are placed within the first cell. The conventional UE is termed UE_1 and communicates with the eNB of this cell, which is termed eNB_1. The two D2D-capable UEs can communicate with each other directly being the transmitting UE termed $D2D_{Tx}$ and the receiving UE termed $D2D_{Rx}$.

Since D2D communication is expected to take place at short distances, we also consider that the D2D pair is inside a limited circular hotspot area of radius R_h within the first cell area. Also notice that the $D2D_{Tx}$ can communicate with $D2D_{Rx}$ via the eNB_1 by using conventional cellular communication instead of D2D mode when necessary.

In the second cell, we model a communication link between one conventional UE, termed UE_2, and the eNB of that cell, termed eNB_2. The main purpose of modeling this link in the second cell is to take into account the intercell interference.

This scenario is illustrated in Fig. 3.3 considering that transmissions occur in the uplink direction, i.e., UE_1 sends data to eNB_1, UE_2 to eNB_2, and $D2D_{Tx}$ sends data to $D2D_{Rx}$ either directly or via the eNB_1. The uplink is the most commonly used link

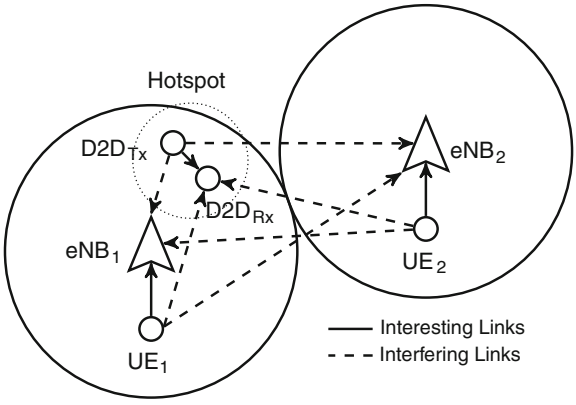

Fig. 3.3 Study scenario for D2D communication mode: uplink case

direction in this chapter; however, conclusions may also be extended for downlink case.

3.2.1.2 Multiple Access, Propagation, and Antenna Modeling

For uplink direction, we consider multiple access scheme based on Orthogonal Frequency-Division Multiple Access (OFDMA) so that the system bandwidth B is divided into a number of subcarriers. As in LTE systems, the subcarriers are spaced of $\Delta f = 15$ kHz and are grouped into PRBs composed of $Q = 12$ adjacent subcarriers. Herein, a PRB is the minimum resource unit that can be allocated to a link for at least one Transmission Time Interval (TTI), which takes 1 ms and transports 14 OFDM symbols.

We also consider that the UEs and eNBs can be equipped with a single omnidirectional antenna or with a standard linear array of omnidirectional antennas [44]. Moreover, we assume that the channel coherence bandwidth is larger than the bandwidth of a PRB, there is the channel is flat fading over a PRB period. Then, on a PRB n we model the channel of the link between a given transmit antenna i and a given receive antenna j by a coefficient $h_{i,j}$, which corresponds to the channel transfer function of the middle subcarrier of the PRB. Consequently, the link between a transmitter t with N_T antennas and a receiver r with N_R antennas on the PRB n is modeled by the $N_R \times N_T$ channel matrix $\mathbf{H}$ given by

$$\mathbf{H} = \begin{bmatrix} h_{1,1} & h_{1,2} & \dots & h_{1,N_T} \\ h_{2,1} & h_{2,2} & \dots & h_{2,N_T} \\ \vdots & \vdots & \ddots & \vdots \\ h_{N_R,1} & h_{N_R,2} & \dots & h_{N_R,N_T} \end{bmatrix} \tag{3.1}$$

where the transmitter, receiver, and PRB indexes are omitted for simplicity of notation. For each transmit-receive antenna pair in Eq. (3.1), the channel coefficient $h_{i,j}$ encompass large scale fading, i.e., average path loss and shadowing, as well as small scale fading, i.e., fast (multipath) fading.

Since the multiple antennas of UEs or eNBs are collocated, the antennas share the same large scale fading. In particular, the average path loss $PL(d)$ expressed in in dB for a transmitter-receiver pair d km apart from each other is modeled as in [2], as

$$PL(d) = \begin{cases} 128.1 + 37.6 \log_{10}(d), & \text{for UEs-BSs links,} \\ 127 + 30 \log_{10}(d), & \text{for D2D}_{\text{Tx}}\text{-D2D}_{\text{Rx}}\text{links,} \end{cases} \tag{3.2}$$

while the shadowing is modeled by a log-normal random variable with standard deviation σ_{sh}.

For the small scale fading, two models were considered: the Zero Mean Circularly Symmetric Complex Gaussian (ZMCSCG) Independent and Identically Distributed (IID) model [39] and the 3GPP Spatial Channel Model (SCM) [8].

3.2.1.3 Signal Model and Precoding/Postcoding

In the most general scenario considered herein, we have a MIMO interference channel with a number L of co-channel links and where each link involves M_T transmit and M_R receive antennas.

On a given PRB, the channel matrix for a link of interest between a receiver k and a transmitter l is denoted by $\mathbf{H}_{k,l}$, which is an $M_R \times M_T$ matrix whose elements $h_{i,j}$ consist in the channel transfer function between the receiver antenna i and transmit antenna j of the MIMO link, as previously described. In our model, the signals sent on this link are filtered, before transmission, by the transmitter l using a transmit matrix $\mathbf{M}_l$ with dimension $M_T \times S_k$, where S_k is the number of transmitted signals (or data streams) sent to user k and $S_k \leq \min(M_T, M_R, \nu)$, where ν is the rank of the channel matrix $\mathbf{H}_{k,l}$.

The filtered signals traverse the channel $\mathbf{H}_{k,l}$, suffer from interference and noise and, at the receiver, are filtered by a receive matrix $\mathbf{D}_k$ with dimension $S_k \times M_R$. Based on these definitions, the input-output relation for the MIMO channel for a certain link is given by

$$\tilde{\mathbf{y}}_k = \mathbf{D}_k \mathbf{y}_k = \mathbf{D}_k (\mathbf{H}_{k,l} \mathbf{M}_l \mathbf{x}_l + \sum_{\substack{l'=1 \\ l' \neq l}}^{L} \mathbf{H}_{k,l'} \mathbf{M}_{l'} \mathbf{x}_{l'} + \boldsymbol{\sigma}_k) \tag{3.3}$$

where $\mathbf{y}_k$ and $\tilde{\mathbf{y}}_k$ are the $S_k \times 1$ prior- and the post-filtering received signal vectors, respectively, $\mathbf{x}_l$ is the $S_k \times 1$ transmit signal vector, and $\boldsymbol{\sigma}_k$ is the $M_R \times 1$ white ZMCSCG noise vector at the receiver i, whose entries have average power σ^2.

Notice that in (3.3), an interferer l' might be a D2D transmitter, as well as a transmitting cellular UE or BS. Similarly, a receiver k might be either a D2D receiver, or a cellular UE or a BS. Still regarding (3.3), it is worth noticing that we consider only linear processing with the postcoding matrices $\mathbf{D}_k$ and precoding matrices $\mathbf{M}_l$ being designed according to a given spatial filtering criterion. In this work, we consider (according to the scenario) one of the following precoding schemes:

- Maximum Ratio Combining (MRC) precoding.
- Singular Value Decomposition (SVD) precoding.
- Zero-Forcing (ZF) precoding.
- Minimum Mean-Square Error (MMSE) precoding.

A more detailed presentation of these (and other) precoding schemes can be found in Chaps. 1 and 9 of this book and references therein.

Finally, each element $y_{k,s}$ of $\mathbf{y}_k$ in (3.3) is associated to the sth, $s = 1, 2, \ldots, S_k$ data stream sent from transmitter l to receiver k. Considering the elements of the transmit signal vectors have unitary power, denoting by $\mathbf{d}_{k,s}$ the sth row of $\mathbf{D}_k$ and denoting by $\mathbf{m}_{l,s}$ the sth column of $\mathbf{M}_l$, the SINR $\gamma_{k,s}$ experienced by sth data stream of receiver k is calculated herein as

$$\gamma_{k,s} = \frac{|\mathbf{d}_{k,s}\mathbf{H}_{k,l}\mathbf{m}_{l,s}|^2}{\sum\limits_{\substack{s'=1 \\ s' \neq s}}^{S_k} |\mathbf{d}_{k,s}\mathbf{H}_{k,l}\mathbf{m}_{l,s'}|^2 + \sum\limits_{\substack{l'=1 \\ l' \neq l}}^{L} \sum\limits_{s'=1}^{S_{l'}} |\mathbf{d}_{k,s}\mathbf{H}_{k,l'}\mathbf{m}_{l',s'}|^2 + \tilde{\sigma}^2}, \tag{3.4}$$

where $\mathbf{m}_{l',s'}$ is the (s')th column of $\mathbf{M}_{l'}$ and $\tilde{\sigma}^2$ is the filtered received noise power.

The data rate $R(\gamma_{k,s})$ of the stream s of a receiver k can be determined by mapping its value to a rate value using a mapping function, such as Shannon's formula [17], or using link level results, such as those provided in [5, 37].

While most of the developments in the previous paragraphs omitted the PRB index and considered a single link of interest, they apply straightforwardly for scenarios with multiple users and multiple resources.

3.2.2 Mode Selection

In a scenario with D2D communications, there are UEs that can communicate directly (assisted or not by the network) instead of using the eNB. The mode selection algorithm is responsible for choosing the adequate mode that D2D-capable UEs shall transmit, which attempts to maximize the total system rate. In this scope, by D2D mode the reader can understand that the D2D communications will occur underlaying the cellular network, and by cellular mode as the UE connected to the pure cellular network. The choice between D2D communication or the standard cellular network is decided by the eNB. The algorithm is applied in a step after the scheduling, because it has to know the number of transmitting users per resource.

The interference is created by the D2D-capable UEs when they transmit in the same resource of cellular UEs, where this mode can be called as shared, because they share the same resource with the cellular link. When the D2D-capable UEs use dedicated resources to transmit, there is no interference with cellular communication since they are using different resources, where this transmission mode is called dedicated. The cellular mode is the well-established mode, where the UEs uses the eNB to transmit and the D2D-capable UEs act as a cellular terminal.

Figures 3.3 and 3.4 illustrate our studied scenario for uplink. There are two circular cells with one eNB placed in each cell center, where the first one has a D2D pair and a cellular UE and the other has only one cellular UE, introduced just to add an extra interfering link. The solid lines represent the interesting links, cellular or D2D, and the dashed ones represent interfering links. The interference can be generated by three sources: the $\mathrm{D2D_{Tx}}$ and the two cellular UEs.

In D2D mode, the user in D2D communication uses the same resources as the cellular user, so that they cause interference to each other. It is assumed that $\mathrm{UE_1}$ transmits to $\mathrm{eNB_1}$, $\mathrm{UE_2}$ transmits to $\mathrm{eNB_2}$ and $\mathrm{D2D_{Tx}}$ transmits to $\mathrm{D2D_{Rx}}$. Therefore, the SINRs and rates are calculated at the $\mathrm{eNB_1}$, $\mathrm{eNB_2}$ and $\mathrm{D2D_{Rx}}$.

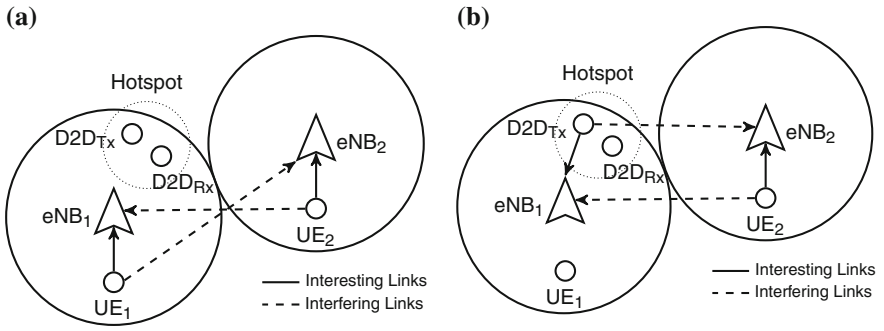

Fig. 3.4 Studied scenario for cellular communication mode: uplink case. **a** Cellular mode in phase 1. **b** Cellular mode in phase 2

In the cellular mode, the D2D terminals can not communicate with each other directly, as such all nodes use orthogonal resources. However, co-channel interference among users of the different cells is assumed. There are two phases in this mode. In phase 1, UE_1 transmits to eNB_1 and UE_2 transmits to eNB_2. In the second phase, only $D2D_{Tx}$ transmits to eNB_1 and UE_2 transmits to eNB_2 again.

In this mode, the SINR and rates are calculated at the eNB_1 and eNB_2. The sum rate in the cellular mode can be considered (roughly) one half of the sum of the rates obtained in each phase. For both D2D and cellular communication modes, Shannon's capacity formula [17] can be used to calculate the rates of the links. As such, the sum rate R^{D2D} for the D2D mode is given by

$$R^{D2D} = R_1^{D2D} + R_2^{D2D} + R_3^{D2D} \tag{3.5}$$

where R_1^{D2D}, R_2^{D2D} and R_3^{D2D} are the rates at the eNB_1, $D2D_{Rx}$ and eNB_2, respectively. While the sum rate R^{cell} in the cellular mode is obtained by averaging the sum rate of the two phases, i.e.,

$$R^{cell} = \frac{1}{2}\left(R_1^{cell} + R_2^{cell}\right) \tag{3.6}$$

where R_1^{cell} and R_3^{cell} are respectively the rates at eNB_1 and eNB_2 in phases 1 and 2.

The sum rate calculated by Shannon's formula might be transformed to a LTE-like rate by multiplying it with the number of PRB in the system, the number of subcarrier in a PRB, the number of symbols in the duration of the TTI and divided by the duration of a TTI. Since the channel bandwidth is 5 MHz, the number of PRBs is 25, the number of subcarriers inside a resource is 12 and the number of symbols is 14, while the duration of TTI considered is 1 ms.

The short distance between the devices allows for direct communication with low transmit power and so contributes to reduce interference and load levels in the system, and consequently improve its performance. Therefore, some regions regarding the

D2D and cellular UE positioning with respect to the eNB can be defined. Denoting by r the distance of a user to its serving eNB, we define two regions represented by discs $R_i \leq r \leq R_o$ limited by an inner radius R_i and outer radius R_o, namely a near eNB region and a near cell-edge region, within which the eNB_1 is placed at the center. The above described regions are defined as:

- Near eNB region: $0.1R_c \leq r \leq 0.15R_c$, where R_i is equal to $0.1R_c$ and R_o equals to $0.15R_c$.
- Near cell-edge region: $0.9R_c \leq r \leq 0.95R_c$, where R_i is equal to $0.9R_c$ and R_o equals to $0.95R_c$.

In order to expand the system to a multicarrier system, a multiuser scenario can be created, in which multiple cellular and D2D users are present. Regarding the distribution of multiple users in the first cell (cell of interest), two cases can be studied. In the first, D2D and cellular users are dropped uniformly within the first cell, then one D2D pair and one cellular pair of UEs are taken to form a so-called group of UEs. One PRB shall be assigned to this group, and it will be shared between the users in the group. A simple but effective technique is to schedule the D2D pair willing to initiate a transmission in the same PRB as the farthest (in terms of distance) pair communicating in cellular mode. Since UEs have limited power transmission, interference to cellular network would also be limited and reduced with distance due to path loss.

In the second, the groups are created considering the existence of a *hotspot*. The idea of the hotspot is to take advantage of the cases where a pair of D2D UEs are closer to each other, far from the eNB, and willing to communicate directly. Hotspots model real situations in which D2D communication is more probable to take place. Thus, in the hotspot case, D2D users are randomly dropped within the hotspot area and cellular users within the whole cell. Then, one D2D pair and one cellular pair of UEs are took to form a group of UEs.

Concerning a practical mode selection, one mode selection algorithm is presented, where the algorithm assumes knowledge only about long term fading of desired and interfering links. The scheme is then compared to an ideal mode selection scheme, which assumes perfect channel information. This algorithm can be applied into a multiuser scenario without loss of generality.

The mode selection scheme is rate-based, which takes into account the rates calculated in the links of the eNB_1. The modes considered are the D2D and the cellular. In the D2D mode, UE_1 transmits to eNB_1, which corresponds to the link 1, and the D2D_{Tx} transmits to the D2D_{Rx}, which corresponds to link 2. In the link 1, the interfering device is D2D_{Tx}, while the device interfering in the link 2 is the UE_1. The closer the UE_1 is to eNB_1 and the further D2D_{Tx} is from eNB_1, higher is the rate for link 1. The same happens to link 2 considering the distance between the D2D pair, i.e., between D2D_{Tx} and D2D_{Rx}, and the distance between UE_1 and D2D_{Rx}.

In the cellular mode, all nodes use orthogonal resources. There are two phases in this mode. In phase 1, UE_1 transmits to eNB_1, UE_2 transmits to eNB_2 while D2D_{Tx} is off. In the second phase, only D2D_{Tx} transmits to eNB_1 while UE_1 is off and UE_2 transmits to eNB_2 again. We consider that the sum rate in the cellular mode is

```
Randomly sort UEs to form a D2D pair
for each cellular pair do
    Calculate the path loss
end for
for each D2D pair do
    Calculate the path loss
end for
Choose an adequate δ_R
for each TTI do
    for each PRB do
        Calculate the rates for R_1^D2D, R_2^D2D, R_1^cell, and R_2^cell
        if R_1^D2D + R_2^D2D ≥ 1/2 (R_1^cell + R_2^cell) + δ_R then
            Choose D2D mode
        end if
    end for
end for
```

Fig. 3.5 Rate-based mode selection algorithm

(roughly) one half of the sum rates obtained in each phase. Without loss of generality, we will not consider UE_2 and eNB_2 of our formulation since the interfering value that comes from UE_2 does not changes significantly our conclusions.

In Fig. 3.5, it is presented the full algorithm. First the UEs are randomly sorted and the D2D pairs are formed. Then, the path loss is calculated for both cellular and D2D UEs. It is necessary to choose an adequate parameter—namely δ_R—which will bias the mode selection decision. The mode selection decision must be done for each TTIs and for each PRB. Then, the rate estimates R_1^{D2D}, R_2^{D2D}, R_1^{cell}, and R_2^{cell} must be computed as:

$$R_1^{\text{D2D}} = \log_2\left(1 + \frac{p_{UE_1}\alpha_1\chi_1}{p_{D2D_{\text{Tx}}}\alpha_3\chi_3 + \sigma^2}\right), \tag{3.7a}$$

$$R_2^{\text{D2D}} = \log_2\left(1 + \frac{p_{D2D_{\text{Tx}}}\alpha_2\chi_2}{p_{UE_1}\alpha_4\chi_4 + \sigma^2}\right), \tag{3.7b}$$

$$R_1^{\text{cell}} = \log_2\left(1 + \frac{p_{UE_1}\alpha_1\chi_1}{\sigma^2}\right), \tag{3.7c}$$

$$R_2^{\text{cell}} = \log_2\left(1 + \frac{p_{D2D_{\text{Tx}}}\alpha_3\chi_3}{\sigma^2}\right), \tag{3.7d}$$

where R_1^{D2D} is the rate calculated for the link 1 between UE_1 and eNB_1 and R_2^{D2D} is the rate calculated for in the link 2 between $D2D_{\text{Tx}}$ and $D2D_{\text{Rx}}$. Besides that, R_1^{cell} is the rate calculated in the link 1 when $D2D_{\text{Tx}}$ is off and R_2^{cell} is the rate calculated in the link 3 between $D2D_{\text{Tx}}$ and eNB_1 when UE_1 is off. In (3.7), p is the transmit power of a specific device, σ^2 is the average noise power, and α and χ are the path loss attenuation and the shadowing found in the following links, related to Fig. 3.3:

- Link 1 $\Rightarrow$ UE_1 to eNB_1.
- Link 2 $\Rightarrow$ $D2D_{\text{Tx}}$ to $D2D_{\text{Rx}}$.

- Link 3 $\Rightarrow$ D2D_{Tx} to eNB_1.
- Link 4 $\Rightarrow$ D2D_{Tx} to UE_1.

Hence, the rate-based mode selection scheme will decide to use D2D communication if the following inequality is satisfied:

$$R_1^{\text{D2D}} + R_2^{\text{D2D}} \geq \frac{1}{2}\left(R_1^{\text{cell}} + R_2^{\text{cell}}\right) + \delta_R \tag{3.8}$$

The variable δ_R is an adjustment factor used in the formulation of the rate-based mode selection scheme to bias its decision. If the relation in (3.8) yields false, then the conventional cellular mode is selected.

3.2.3 Resource Block Allocation

In general, a scheduler may be divided in two main parts: resource allocation and resource assignment (or resource block allocation and resource block assignment in OFDMA-based systems). The resource allocation is responsible for defining which flows are scheduled and determine their required data rates at a specified point in time; while the resource assignment defines which resources are actually assigned to the selected flows. From this point on, the resource allocation and assignment is generally referred as scheduling or simply resource block allocation.

While in D2D communications as an underlaying network of the existing cellular one, the mode selection must be considered. In brief, it refers to the choice of mode to transmit: cellular or direct mode. In cellular mode, the communication link is establish through the radio access network, i.e., the common cellular links, while a direct communication is a device-to-device link establishment (for details on mode selection see Sect. 3.2.2).

The mode selection shall consider both links' quality (toward the eNB and the UE) in different interference situations, namely when a D2D pair reuses the same resources as the cellular UEs (shared manner) or, eventually, when the D2D communication uses dedicated resources (dedicated manner).

Regardless the type, shared or dedicated, scheduling is always present in a multiuser and multicell network due to scarcity and great value of electromagnetic spectrum, that must be shared among all UEs in the network. Yet considering the operator's licensed spectrum, it seems more attractive to properly reuse PRBs for D2D communications and, therefore, increase the spectral efficiency.

However, following a shared type, the network must cope with new intracell (or co-channel) interference situations, in addition to the already present intercell interference, i.e., the orthogonality between the UEs is no longer kept. Thus, the scheduling process assumes great importance: distribute resources among all (cellular and D2D) UEs while keeping interference at acceptable and controllable values.

Next, two well-known scheduling algorithms—Rate Maximization (RM) and Round Robin (RR)—are briefly discussed. The main objective of RM is to max-

imize the total systems' data rate. Considering a multiuser and multicell system using the OFDMA access technique, the solution for this problem is quite simple: the algorithm assigns each PRB to the UE for which the highest channel gain on that PRB is verified. The algorithm continues to assign PRBs to the respective UEs with the best channel until all PRBs have been assigned [30]. As such, UEs with worst channel gain may suffer from starvation, i.e., never be selected for transmission.

However, since in D2D communications as an underlaying network we deal most of the times with groups—schedule a D2D pair along with an already scheduled cellular UE or cellular pair—variations of the RM algorithm shall be considered. Therefore, the main idea is to calculate the rate of groups sharing the same PRBs in downlink and uplink and then choose the group that maximizes the desired rate, as presented in Fig. 3.6. The maximization scheduling policies may be one of the following:

- The uplink rate of cellular mode.
- The uplink rate of D2D mode.
- The downlink rate of cellular mode.
- The downlink rate of D2D mode.
- The sum of downlink and uplink rates for the cellular mode.
- The sum of downlink and uplink rates for the D2D mode.

Figure 3.7 presents the matching between cellular and D2D pairs: $\{C_1, C_2, \ldots, C_N\}$ represent the N different cellular pairs; $\{D_1, D_2, \ldots, D_N\}$ represent the D2D pairs that will match with the cellular ones; and $\{G_1, G_2, \ldots, G_N\}$ is the set of defined groups. Pairs are organized according to the path loss, where the cellular pairs are in crescent order ($PL_{C_1} < PL_{C_2} < \cdots < PL_{C_N}$) and D2D pairs are in decrescent order ($PL_{D_1} > PL_{D_2} > \cdots > PL_{D_N}$). Thus, the first group G_1 has the

```
1: Randomly sort UEs to form a cellular pair
2: Randomly sort UEs within hotspot to form a D2D pair
3: for each cellular pair do
4:     Calculate the path loss
5: end for
6: for each D2D pair do
7:     Calculate the path loss
8: end for
9: Sort the path loss lists
10: Match the path loss lists in reverse order of each other forming a group of two pairs (see
    Fig. 3.7)
11: for each TTI do
12:     for each PRB do
13:         Select the group with highest channel
14:         Perform link adaptation for UEs of selected group
15:     end for
16: end for
```

Fig. 3.6 Algorithm for the resource block allocation using the RM scheduler

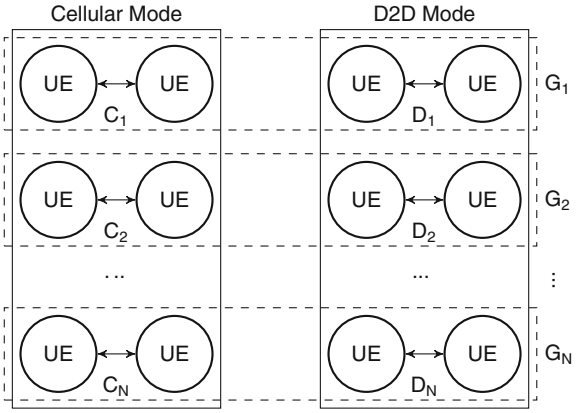

Fig. 3.7 Grouping according to the path loss of cellular and D2D pairs, where $PL_{C_1} < PL_{C_2} < \cdots < PL_{C_N}$ and $PL_{D_1} > PL_{D_2} > \cdots > PL_{D_N}$

highest combined channel gain, then the second G_2, and so on. Furthermore, the path loss is measured against each transmitting device and the respective serving eNB.

The principle behind RR, contrary to RM, is to be fair by assigning the same number of PRBs to every group of UEs. The scheduler generates a list with all suitable groups of UEs and randomly assigns one PRB to each group following the list order. The process starts again from the beginning of the same list once all groups received PRBs, as shown in Fig. 3.8.

Although the groups tend to have the same number of PRBs, they do not reach the same data rate, since PRBs allocated to different groups will suffer different propagation conditions according to their position in the cell.

```
1: Randomly sort UEs to form a cellular pair
2: Randomly sort UEs within hotspot to form a D2D pair
3: for each cellular pair do
4:     Calculate the path loss
5: end for
6: for each D2D pair do
7:     Calculate the path loss
8: end for
9: Sort the path loss lists
10: Match the path loss lists forming a group of two pairs (see Fig. 3.7)
11: for each TTI do
12:     for each group do
13:         Randomly select a PRB
14:         Perform link adaptation for UEs of the group
15:     end for
16: end for
```

Fig. 3.8 Algorithm for the resource block allocation using the RR scheduler

3.2.4 Power Allocation

In the following paragraphs we describe the transmit power control algorithms whose performance is evaluated in this chapter considering cellular and D2D communications. Let us focus on the algorithm proposed in Ref. [16] for the uplink of multicell MIMO systems, which considers a fixed target SINR value, and on extensions of this algorithm considering variable SINR values. In all cases, we are interested in providing certain QoS levels while minimizing the total transmit power.

Considering the definitions in Sect. 3.2.1 and organizing in the form of a vector $\mathbf{p_k} = \left[p_{k,1} \; p_{k,2} \; \dots \; p_{S_k} \right]$ the transmit powers allocated to each stream s of the UE k, we desire to solve the problem

$$\{\mathbf{p}_1^\star, \dots, \mathbf{p}_K^\star\} = \underset{\{\mathbf{p}_1, \dots, \mathbf{p}_K\}}{\arg\min} \sum_{k=1}^{L} \sum_{s=1}^{S_k} p_{k,s} \tag{3.9a}$$

$$\text{subject to} \quad \gamma_{k,s} \geq \Gamma_{k,s}, \; \forall k \in \{1, \dots, K\} \text{ and } s \in \{1, \dots, S_k\}, \tag{3.9b}$$

$$\sum_{s=1}^{S_k} p_{k,s} \leq p_k, \; \forall k \in \{1, \dots, K\}, \tag{3.9c}$$

$$p_{k,s} \geq 0, \; \forall k \in \{1, \dots, K\} \text{ and } s \in \{1, \dots, S_k\}, \tag{3.9d}$$

where $\Gamma_{k,s}$ is target SINR of the stream s of the UE k and p_k is the maximum transmit power of UE k.

The algorithm of Ref. [16], which is termed hereafter Equal Power Allocation (EPA) algorithm, and their referred extensions are based on interference functions which represent the effective interference that an UE (or UE's stream) must overcome to attain its target SINR [50]. The approach of these algorithms is similar to that proposed in Ref. [41], in which precoding and power allocation are optimized alternately.

For the power control algorithms in this chapter, the precoding matrices of (3.3) and (3.4) can be written as $\mathbf{M}_k = \mathbf{W}_k \sqrt{\mathbf{P}_k}$, where $\mathbf{W}_k$ is an $M_T \times S_k$ normalized precoding matrix whose columns have unitary norm and $\mathbf{P}_k = \text{diag}(\mathbf{p}_k)$ is an $S_k \times S_k$ real, diagonal, power allocation matrix which allocates the power $p_{k,s}$ to the sth stream of receiver k while fulfilling the constraint $\text{tr}(\mathbf{P}_k) \leq p_k$ in order to obey (3.9c).

Considering that perfect CSI is available at each transmitter and receiver, using (3.4), and assuming equality in (3.9c), one can express

$$p_{k,s} = \Gamma_{k,s} \frac{\left(\sum\limits_{\substack{s'=1 \\ s' \neq s}}^{S_k} p_{l,s'} |\mathbf{d}_{k,s} \mathbf{H}_{k,l} \mathbf{w}_{l,s'}|^2 + \sum\limits_{\substack{l'=1 \\ l' \neq l}}^{L} \sum\limits_{s'=1}^{S_{l'}} p_{l',s'} |\mathbf{d}_{k,s} \mathbf{H}_{k,l'} \mathbf{w}_{l',s'}|^2 + \tilde{\sigma}^2 \right)}{|\mathbf{d}_{k,s} \mathbf{H}_{k,l} \cdot \mathbf{w}_{l,s}|^2}, \tag{3.10}$$

$$= I_{k,s}(\mathbf{P}_1, \ldots, \mathbf{P}_K, \mathbf{W}_1, \ldots, \mathbf{W}_K),$$

where $I_{k,s}(\mathbf{P}_1, \ldots, \mathbf{P}_K, \mathbf{W}_1, \ldots, \mathbf{W}_K)$ is a standard interference function [15, 18, 36, 38, 41, 50]. Then, considering this model, the power control algorithms of this chapter, including that of Ref. [16], can be described as particular cases of the algorithm in Fig. 3.9, for which particular forms are employed to compute $\mathbf{P}_k$ and $\mathbf{W}_k$.

The basic idea of the EPA algorithm is to allocate the same power to each transmit antenna and then provide the worst stream of the UE with a target SINR $\Gamma_{k,s} = \Gamma_t$. If the worst stream achieves its target, all streams of the UE will experience acceptable QoS. Moreover, by taking only the worst stream, the EPA reduces the multiuser MIMO power control problem to a multiuser Multiple-Input-Single-Output (MISO) one, since effectively only the worst channel of each co-channel UE is taken into account by the power control algorithm.

For the EPA algorithm, one sets $\mathbf{W}_k^{(0)} = \mathbf{I}$ and $\mathbf{P}_k^{(0)} = \frac{p_k}{S_k}\mathbf{I}$ in the algorithm of Fig. 3.9. Then, using the interference function in (3.10), the effective interference of each stream s of receiver k is computed considering MMSE precoding at the receiver. The diagonal elements $\mathbf{W}_k^{(t)}$ are then updated as the effective interference value of each stream s normalized by the sum of the effective interference of the S_k

1: Set the initial iteration $t \leftarrow 0$
2: Calculate precoding matrices $\mathbf{W}_k^{(t)} = \mathbf{W}_k^{(0)}, \forall k$
3: Set initial power allocation matrices $\mathbf{P}_k^{(t)} \leftarrow \mathbf{P}_k^{(0)}, \forall k$
4: **repeat**
5: Let $t \leftarrow t + 1$
6: **for** $k = 1 \rightarrow K$ **do**
7: Update $\mathbf{W}_k$ according to the selected precoding scheme
8: **end for**
9: **for** $k = 1 \rightarrow K$ **do**
10: **for** $s = 1 \rightarrow S_k$ **do**
11: Update $p_{k,s}^{(t)} = I_{k,s}\left(\mathbf{P}_1^{(t-1)}, \ldots, \mathbf{P}_K^{(t-1)}, \mathbf{W}_1^{(t-1)}, \ldots, \mathbf{W}_K^{(t-1)}\right)$
12: **end for**
13: **end for**
14: **until** $\left| \frac{p_{k,s}^{(t)} - p_{k,s}^{(t-1)}}{p_{k,s}^{(t-1)}} \right| \leq \eta, \forall k, s$ and $\eta \ll 1$
15: Set optimum $p_{k,s}^{\star} = p_{k,s}^{(t)}, \forall k, s$

Fig. 3.9 Power allocation and precoding algorithm

streams of UE k, so that $\mathrm{tr}\left(\left(\mathbf{W}_k^{(t)}\right)^H \mathbf{W}_k^{(t)}\right)$ remains equal to S_k but its diagonal elements are no longer equal. In this way $\mathbf{W}_k^{(t)}$ mainly distributes the power among the streams. In the sequel, the powers $p_{k,s}^{(t)}$ for each stream s of UE k are computed, but only the highest power value $p_{k,s}^{\max}$ is preserved. Then, one makes $\mathbf{P}_k^{(t)} = p_{k,s}^{\max}\mathbf{I}$, so that the $\mathrm{tr}\left(\left(\mathbf{W}_k^{(t)}\sqrt{\mathbf{P}^{(t)}}_k\right)^H \mathbf{W}_k^{(t)}\sqrt{\mathbf{P}^{(t)}}_k\right)$ remains smaller than or equal to p_k, thus respecting the power constraint in (3.9c). A more detailed description of the EPA algorithm is out of the scope of this chapter, but can be found in Ref. [16].

While being based on interference functions [50], which ensure convergence whenever the target SINR values are feasible (i.e., whenever target SINR values can be attained with the existing channel conditions), the EPA algorithm assumes a fixed receive precoding scheme (namely MMSE); employs real, diagonal, normalized precoding matrices $\mathbf{W}_k$; and considers a fixed SINR Γ_t for the worst stream. These fixed assumptions might affect the feasibility (probability that the target SINR are feasible) and the power consumption of the UEs in the uplink. In a feasible case, the worst stream of a UE will attain an SINR exactly equal to Γ_t while the other streams will experience in-excess QoS. Therefore, if not only the worst, but all streams of a UE were to attain SINR values equal to Γ_t, the UE would expend less power as well as generate less interference. With this motivation, we have extended the EPA algorithm to an Adaptive Power Allocation (APA) algorithm in which all streams of a UE k are supposed to attain the same fixed target SINR value Γ_t. Besides that, we employ the modeling described in this section which supports different linear precoding schemes at transmitters/receivers whose effect is captured in the effective interference functions.

Because, in general, fixed target SINR values might compromise the feasibility of the power allocations, we further improved the APA algorithm to consider variable target SINR values. For this extension, we followed the model proposed in Refs. [18, 28, 36, 38] which determines the target SINR value $\Gamma_{k,s}^{(t)}(p_{k,s}^{(t)})$ as a linear decreasing function in dB scale of the power $p_{k,s}^{(t)}$ demanded by the stream s of UE k. In this case, the target SINR $\Gamma_{k,s}^{(t)}$ of a stream s of a receiver k can vary between a maximum SINR value $\Gamma_{\max}$ and a minimum SINR value $\Gamma_{\min}$ as its demanded power $p_{k,s}^{(t)}$ goes from a minimum value $p_{\min}$ to a maximum $p_{\max}$, respectively. Thus, when a stream increases its demanded power, its target SINR will lowered and, as a consequence, the likelihood that all co-channel links are supported (feasible power allocation) increases. In this way, the links with better channel conditions are likely to operate with high SINR and low power while links with bad channel conditions will trade the operation at lower SINR values for the sake of the efficiency of the other co-channel links. The mapping from demanded power to target SINR is illustrated in Fig. 3.10 in which the indicated SINR and power values are expressed in dB and dBm, respectively.

According to this model [18, 28, 36, 38], the target SINR can be expressed as

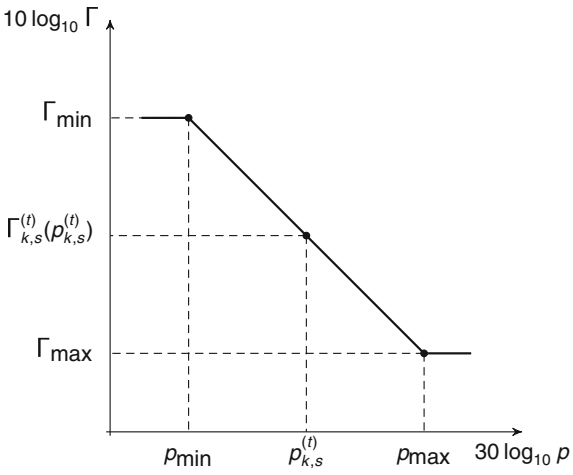

Fig. 3.10 Power to target SINR mapping

$$\Gamma_{k,s}^{(t)}(p_{k,s}^{(t)}) = \min\left(\Gamma_{\max}, \max\left(\Gamma_{\min}, \left(\Gamma_{\max}\frac{p_{k,s}^{(t)}}{p_{\min}}\right)^{\rho}\right)\right), \text{ where} \tag{3.11}$$

$$\rho = \frac{\log_{10}(\Gamma_{\min}/\Gamma_{\max})}{\log_{10}(p_{\max}/p_{\min})}.$$

Finally, using the SINR in (3.4) and the interference function of (3.10), the power allocation is in the APA algorithm is adapted to

$$p_{k,s}^{(t+1)} = p_{k,s}^{(t)}\left(\frac{\Gamma_{k,s}(p_{k,s}^{(t)})}{\gamma_{k,s}^{(t)}}\right)^{\beta_k} \tag{3.12}$$

where $0 < \beta_k \leq 1$ is a control parameter. A more detailed description of this approach can be found in Refs. [18, 28, 36, 38].

3.2.5 User Grouping

In D2D communications as an underlaying network, the group could be formed by a D2D pair along with an already scheduled cellular UE. The resources shall be allocated to each user in the group, where the users shall be chosen based on some grouping metric which measure the compatibility among the D2D pair and the cellular UE. We propose two grouping metrics in this mixed D2D and cellular environment. In the first strategy, we propose a method to create groups of UEs following a distance-based approach. In the second one, we extend the successive

1: Randomly sort UEs to form a cellular pair
2: Randomly sort UEs within hotspot to form a D2D pair
3: **for** each cellular pair **do**
4: Calculate the path loss
5: **end for**
6: **for** each D2D pair **do**
7: Calculate the path loss
8: **end for**
9: Initialization: p, n
10: **for** $\tilde{p} = 1 \rightarrow p$ **do**
11: Select the highest channel gain among cellular users
12: **for** $\tilde{n} = 1 \rightarrow n$ **do**
13: Select the smallest channel gain among D2D users
14: **end for**
15: Form a group with the pairs to which the UEs of step 11 and 13 belong
16: **end for**

Fig. 3.11 Distance-based grouping

allocation method of spatial channels proposed in Ref. [43] to a wireless network where D2D and cellular users are reusing the same resources.

The first method is based on distance studies about the mode selection, presented in Sects. 3.3.1 and 3.3.2. These studies have helped to identify at which positions of D2D and cellular users configure situations where D2D communication can increase the overall system capacity. Considering the uplink case, the conducted analyses indicate that when the transmitting UE in the cellular pair is near the serving eNB and a D2D pair near the cell-edge are sharing resources, the achieved rates by D2D mode are considerably better than those achieved in cellular mode.

The distance-based grouping algorithm shows the principle of the distance-based users grouping and the procedure is depicted in Fig. 3.11. First the UEs are randomly sorted and the D2D pairs are formed. Then, the path loss is calculated for both cellular and D2D UEs. Then, in order to form a group of UEs, the algorithm selects the UE with highest channel gain to the eNB among all cellular UEs. In the sequel, the D2D UE with smallest channel gain to eNB is chosen.

The pairs (cellular and D2D ones) to which these UEs belong are selected to share the same PRB. This last loop is repeated until the number of D2D users specified by n is reached, so as to select n D2D pairs to share the resource with the cellular UE. The process continues until all the UEs in the system are organized in groups creating a number p of groups. The fundamental idea here is to form groups of favorable UEs to attain the resource reuse gain arising from the utilization of D2D communication. When considering multiple antenna configurations, the channel gain used in this algorithm considers only the long term fading component thus rendering a scalar.

Differently of Ref. [43] where the downlink of cellular network is considered, we adequate the idea of successive allocation of spatial subchannels to the uplink case with D2D communication. The aim is to select a set of virtually decoupled subchannels over which the capacity can be maximized.

1: Randomly sort UEs to form a cellular pair
2: Randomly sort UEs within hotspot to form a D2D pair
3: **for** each cellular pair **do**
4: Calculate the path loss
5: **end for**
6: **for** each D2D pair **do**
7: Calculate the path loss
8: **end for**
9: Initialization: n, $\tilde{n} = 1$, $\mathbf{T}_{\tilde{n}} = \mathbf{I}_{t_x}$
10: Select the cellular UE $c^{\star} = \arg\max_{c} \{\|\mathbf{h}_c\|_2\}$
11: **repeat**
12: Select the D2D UE $k_{\tilde{n}}^{\star} = \arg\max_{k} \left\{\|\mathbf{h}_k^T \mathbf{T}_{\tilde{n}}\|_2\right\}$
13: $\mathbf{T}_{\tilde{n}+1} = \mathbf{T}_{\tilde{n}} - \dfrac{\mathbf{T}_{\tilde{n}} \mathbf{h}_{k_{\tilde{n}}^{\star}}^{*} \mathbf{h}_{k_{\tilde{n}}^{\star}}^{T} \mathbf{T}_{\tilde{n}}^{H}}{\left\|\mathbf{h}_{k_{\tilde{n}}^{\star}}^{T} \mathbf{T}_{\tilde{n}}\right\|_2^2}$
14: $\tilde{n} = \tilde{n} + 1$
15: **until** $\tilde{n} > n$ {$\mathbf{h}_k$ is the channel matrix of the user k, $n \leq \lfloor t_x / r_x \rfloor$, t_x is the number of transmit antennas, and r_x is the number of receive antennas}

Fig. 3.12 Successive allocation-based grouping

The Fig. 3.12 shows how a group of UEs is formed. Similarly to the distance-based one, first the UEs are randomly sorted and the pairs are formed. Then, the path loss is calculated for both cellular and D2D UEs. After that, the algorithm chooses the cellular user with highest channel gain to the eNB, similarly as in the distance-based. In the sequel, in the first loop the D2D-capable UE with highest channel gain is chosen to share resources with the cellular pair. In the second loop, considering the null space of the channel of the first D2D UE, the second D2D user is chosen to be the one that exhibits the highest gain in this subspace, i.e., after projecting its channel on the null space of the previously selected D2D-capable UE. In the 12th step, the D2D-capable UE that exhibits the highest gain within the subspace orthogonal to the channels of previously selected D2D-capable UEs is selected.

3.3 Performance Evaluation

In Sect. 3.2 we presented the basis for the studied D2D communication RRA algorithms. In this section, we provide the performance evaluation for those algorithms and their main assumptions. For the simulations, the main parameters are listed in Table 3.1 and were mostly taken from Refs. [1–8, 39]. However, for specific simulations, some parameters had to be tuned, which is properly referenced when necessary. Moreover, the results presented in the following paragraphs considered a large number of Monte Carlo realizations.

It is important to observe that all the rates presented in the following are meant for a comparative study, and shall not be confused with the practical performance

Table 3.1 Simulation parameters

Parameter	Value
System central frequency	2 GHz
System bandwidth	5 MHz (in UL and DL)
Number of PRB	25 (in UL and DL)
Subcarrier bandwidth	15 kHz
Number of subcarriers per PRB	12
Path loss model for cellular links	$128.1 + 37.6 \log_{10}(d)$, d in km
Path loss model for D2D links	$127 + 30 \log_{10}(d)$, d in km
Log-normal shadowing standard deviation	8 dB
Channel model	ZMCSCG IID model and 3GPP SCM typical urban micro model
Cell radius	250 m
Inter-site distance	500 m
Hotspot radius	25 m, 50 m, and 100 m
Noise power	−116.4 dBm
Total transmit power	24 dBm for UEs and 43 dBm for eNBs
CSI knowledge	Perfect
Spatial filtering	MRC, SVD, ZF, and MMSE
Number of Tx and Rx antennas	1×1, 2×2, and 2×4
Total simulation time	1 TTI

obtained in the LTE network, since there are parameters/variables that were not considered in our simulations.

3.3.1 Mode Selection

In the following text we analyze the scenarios proposed in Sect. 3.2.2, where the D2D mode can improve the total system rate and the ones which the usage of D2D communication is a challenge. In every run, we kept fixed the positions of the two eNBs, namely eNB_1 and eNB_2, and the cellular device from the interfering cell, namely UE_2, as shown in Fig. 3.3. The D2D pair, namely the D2D_{Tx} and D2D_{Rx} nodes, and the cellular device UE_1 are not placed randomly, i.e., they are placed in a specific position, and then the positions are varied following a fixed step in each snapshot. Moreover, for each snapshot we calculate the system sum rate for the D2D and cellular modes based on (3.5) and (3.6), respectively. The system sum rate is the sum of all rates in the system, considering both cells and all users.

In order to do this, we vary their positions in steps of 20 m in x and y directions starting from a minimum distance of 10 m from eNB_1. Additionally, we do not allow any two devices, UE_1, D2D_{Tx} and D2D_{Rx}, to sit on the same position at the same time. Several possible combinations of positions for these three devices inside the cell (centered in eNB_1) are considered and in this way we can sample several

possible configurations over the whole interesting covered area by the first cell and characterize the performance of D2D and cellular communication modes.

The first main result shows the percentage of cases in which the system sum rate is larger when D2D is enabled. In Fig. 3.13 we show results for cases in which the D2D mode outperforms the cellular mode in terms of rate, keeping the exact same positions of the nodes for both modes. In this case, it is possible to measure how much the D2D can really improve the sum rate of the system. The dashed curve is the Cumulative Distribution Function (CDF) of the sum rate obtained when the D2D mode is enabled and the solid curve is the CDF of the sum rate obtained when the cellular mode is performed at the same positions. We can observe that half of cases show a relative gain in the sum rate of approximately 32 % when D2D communication is enabled.

The result expressed in Fig. 3.14a shows the CDF of the sum rate when the rates of cellular mode outperforms those obtained in the D2D mode. In this case, the dashed curve is the CDF of the sum rate obtained when the D2D mode is enabled and the solid curve is the CDF of the sum rate obtained when the cellular mode is enabled. We can observe that in half of cases when D2D is enabled the relative gain of the cellular mode is around 70 %. This result just illustrates that the D2D communication should not be applied all the time, but only in some favorable conditions, e.g., when the distance in D2D pair is small and when they are in the cell-edge. Otherwise, its utilization can bring losses to the system due to mutual interference.

Moreover, in Fig. 3.14b we show a result concerning the rates obtained when only the cellular mode is enabled and also another curve illustrating the rates if a mode selection algorithm is applied. This mode selection curve represents the best rates found in each case, considering cellular and D2D modes. We can conclude that if the D2D is chosen in some of the occasions commented before, there will be a gain in the system sum rate, implying that the interference created by the usage of D2D communication is limited by the mode selection algorithm.

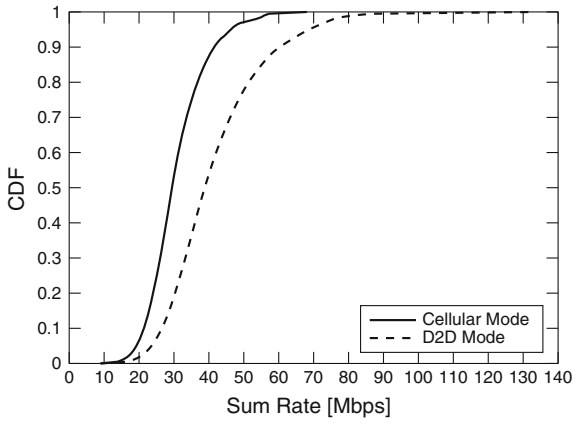

Fig. 3.13 Sum rates of D2D and cellulars mode at the same positions

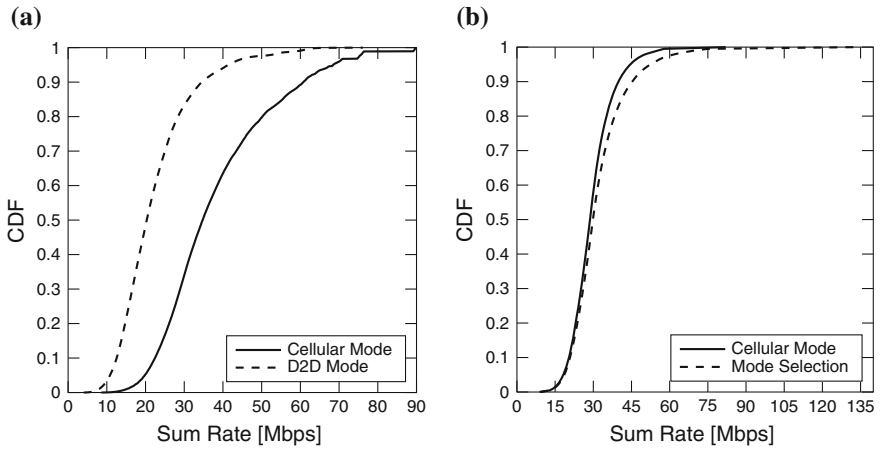

Fig. 3.14 Comparison between a case where D2D communication can bring losses with one that improves the system sum rate. **a** Cellular mode outperforms D2D mode. **b** Cellular mode and mode selection

In order to take some conclusions concerning distances, we investigate in which possible cases the D2D mode would bring a gain in the rate as function of the main distances involved in the problem. In Fig. 3.15 it is shown to some distances the percentage of cases in which D2D mode outperforms the cellular mode. The main distance to be analyzed is between $D2D_{Tx}$ and the $D2D_{Rx}$. It is important to remember that the larger possible distance between them happens when they are diametrically opposed, which is, in this work, 500 m. The Fig. 3.15 shows that when this distance, represented with the dashed line, is around 150 m, the percentage of cases in which D2D mode outperforms the cellular mode is larger than 50 %. It is important to observe that this distance can substantially influence the result. As an example, when this distance is less than around 50 m, the percentage of cases in which D2D mode outperforms becomes approximately 90 %.

The distance of UE_1 from eNB_1 should be also analyzed. A similar behavior is expected once this link is also of interest in the calculation of the system sum rate. In Fig. 3.15 it is also possible to see that when this distance is around 100 m the percentage of success of the D2D mode is larger than 50 %. It is important to remember that the largest possible distance between eNB_1 and any device located inside a cell centered at eNB_1 is 250 m.

Now, we make performance analyses conditioned to specific positions of UE_1, $D2D_{Tx}$ and $D2D_{Rx}$. This approach has been chosen to help determining at which positions of UE_1 conditioned to the distance between $D2D_{Tx}$ and $D2D_{Rx}$ configures scenarios in which D2D communication can increase the system sum rate using uplink resources. For that purpose, we have made two different analysis: without and with restriction concerning the distances between $D2D_{Tx}$ and $D2D_{Rx}$. In the case without restriction, UE_1 is placed into one of the two different regions defined

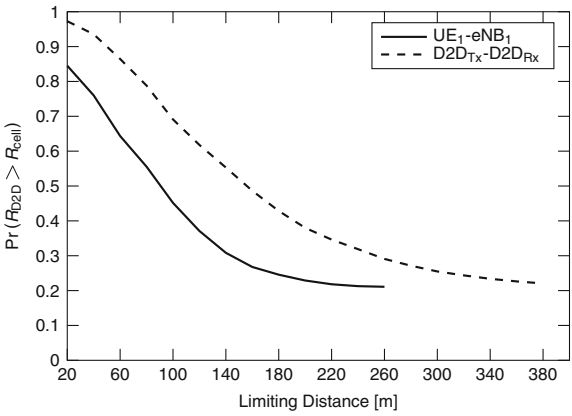

Fig. 3.15 Limiting distance between $D2D_{Tx}$-$D2D_{Rx}$ and UE_1-eNB_1

in Sect. 3.2.2—near cell-edge and near eNB—and the distance between $D2D_{Tx}$ and $D2D_{Rx}$ is not restricted. In the case with restriction on the distance between $D2D_{Tx}$ and $D2D_{Rx}$, UE_1 is still placed into one of the two different regions and we impose that the distance between $D2D_{Tx}$ and $D2D_{Rx}$, termed $d_{Tx\text{-}Rx}$, must be smaller or equal to 50 m.

In Fig. 3.16 we find the sum rate CDF of the D2D and the cellular modes for the median values, both in near eNB and near cell-edge regions. When UE_1 is close to eNB_1, the sum rates of the D2D mode still show a gain of at least 4.2 Mbps in about 30 % of the cases and, in 10 % of the cases, such gain can reach 8.4 Mbps. On the other hand, when UE_1 is close to the cell-edge, the cellular mode can reach better sum rates than D2D mode in all cases. Without the restriction between $D2D_{Tx}$ and $D2D_{Rx}$, the $D2D_{Tx}$ can be far from $D2D_{Rx}$ or even the $D2D_{Rx}$ can be close to the UE_1, increasing the interference to UE_1, thus reducing the performance of D2D mode for both regions.

In Fig. 3.17 it is presented the D2D gain with distance. We define $\Pr(R_{D2D} > R_{cell})$ as the probability that the rate of D2D mode is greater than the rate of the cellular mode. Hence, we can see how this probability varies when $d_{Tx\text{-}Rx}$ and the distance between UE_1 and $D2D_{Rx}$, termed $d_{UE_1\text{-}Rx}$, increases. As such, in Fig. 3.17a, UE_1 is in the near eNB region and therein the smallest probability of the rate of the D2D mode surpassing the rate of the cellular mode is 30 %, even when $D2D_{Tx}$ is far from the $D2D_{Rx}$ and the UE_1 is near the $D2D_{Rx}$. In Fig. 3.17b we can see that when UE_1 is in the near cell-edge region the probability greatly varies mainly for $d_{Tx\text{-}Rx}$.

From Figs. 3.17a, b we can conclude that when the $d_{Tx\text{-}Rx}$ is smaller than 50 m, the probability that the rate of the D2D mode is greater than the rate of the cellular mode is at least 90 % and when the $d_{UE_1\text{-}Rx}$ increases, so does the probability that the rate of D2D mode is greater than the rate of cellular mode.

Until now, we have compared the D2D and cellular modes without restricting the distance between $D2D_{Tx}$ and $D2D_{Rx}$, named $d_{Tx\text{-}Rx}$. In the sequel, we will evaluate a scenario which restricts the D2D positioning and see its improvements against an

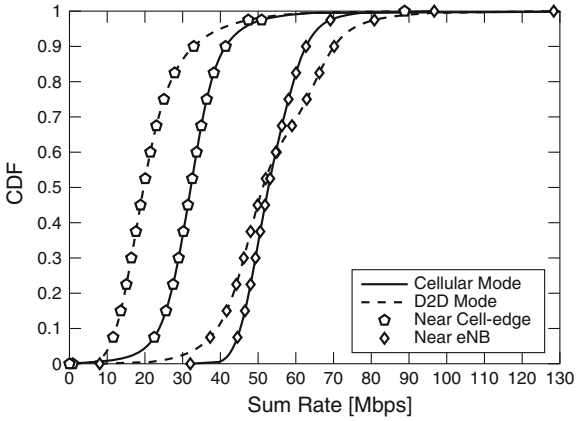

Fig. 3.16 Sum rates in D2D and cellular modes for each set of UE_1, $D2D_{Tx}$ and $D2D_{Rx}$ positions: median

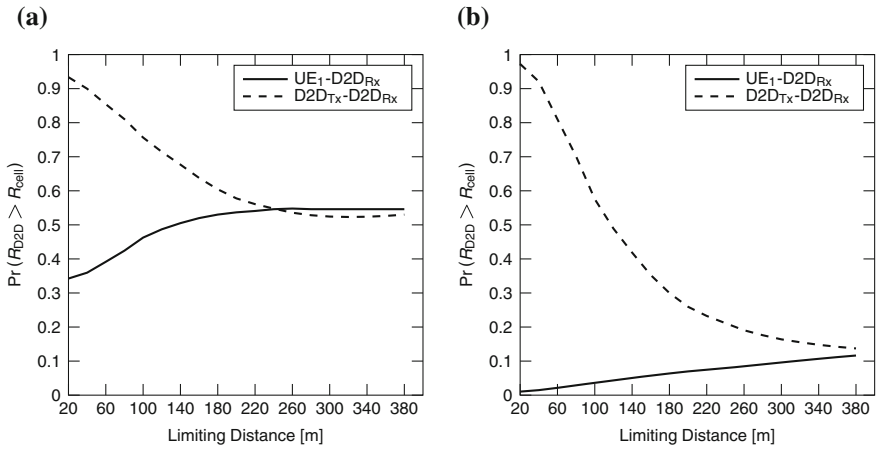

Fig. 3.17 Variation of the D2D gain with distance. **a** UE_1 near eNB. **b** UE_1 near cell-edge

unrestricted scenario. In Figs. 3.18, 3.19, and 3.20 we compare the sum rate CDF obtained in the cellular mode with that obtained in the D2D mode for the situations in which $D2D_{Tx}$ and $D2D_{Rx}$ are distant from each other at most by 50 m considering the 10th percentile, the median and the 90th percentile of rate values, respectively.

The analysis of the 10th percentile depicted in Fig. 3.18 aims to study the behavior of the D2D mode when we consider the worst 10 % sum rates. The near eNB region shows a relative gain in the sum rate of at least 40 % in half of cases when D2D mode is enabled, while near cell-edge region shows a gain of at least 70 % in half of cases. Even considering this, the D2D mode provides a better performance compared to the cellular mode, except for 11 % of the cases in the near eNB region, where the cellular mode outperforms the D2D mode.

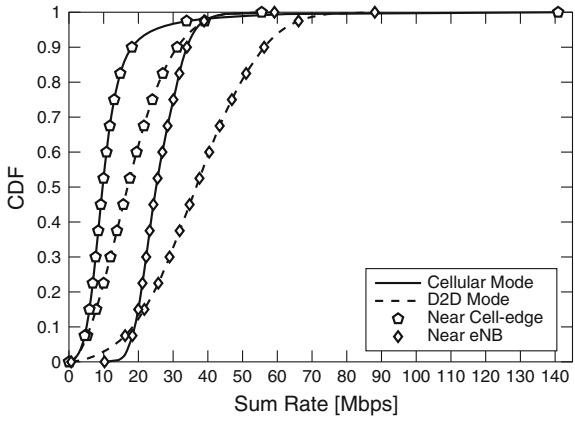

Fig. 3.18 The worst 10 % rates when $D2D_{Tx}$ and $D2D_{Rx}$ are distant less than 50 m from each other: 10th percentile

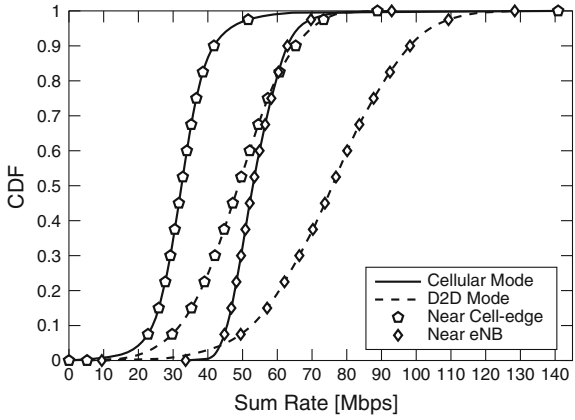

Fig. 3.19 Sum rates when $D2D_{Tx}$ and $D2D_{Rx}$ are distant less than 50 m from each other: median

Regarding the median values, in Fig. 3.19 we can see that when UE_1 is in the near eNB region the rates are greater than when UE_1 is in the near cell-edge region. Moreover, comparing Figs. 3.16 and 3.19, we have shown that not only the near eNB region had better results, but also the near cell-edge region, which did not show good results for the use of D2D in Fig. 3.16. The near eNB region shows a relative gain of at least 40 % in half of cases, while near cell-edge region shows a relative gain of at least 50 % in half of cases.

In Fig. 3.20 the analysis of the 90th percentile is performed, which aims to study the behavior of the D2D mode when we consider the best 10 % sum rates. The two regions show a gain when D2D mode is enabled, but the near eNB region still shows a higher gain. The near eNB region shows a gain of at least 30 % in half of cases, while near cell-edge region shows a gain of at least 30 % in half of cases. Considering the better rates, the cellular mode outperforms the D2D mode in the near eNB region only in 1 % of the cases, while in the near cell-edge region the D2D mode always outperforms the cellular mode. Therefore, when UE_1 is in the near eNB region the

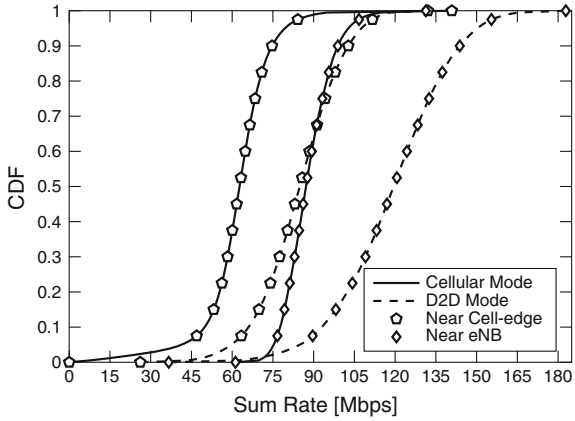

Fig. 3.20 The best 10 % rates when $D2D_{Tx}$ and $D2D_{Rx}$ are distant less than 50 m from each other: 90th percentile

rates are greater than when UE_1 is in the near cell-edge region. Moreover, when we restrict the $d_{\text{Tx-Rx}}$, the rates achieved by the D2D mode are greater even in the near cell-edge region, where without restriction the rates were always lower than the cellular mode.

We compare now the practical scheme of mode selection previously described, namely rate-based mode. The goal is to determine how different are the practical scheme and the ideal mode selection, which considers perfect CSI. Besides that, we compare these two mode selection algorithms with the results obtained considering just the cellular mode, and thus we can observe the gains added by D2D communication. The analyzed Tx × Rx antenna configurations are 1×1, 2×2, and 4×4.

Differently from the results presented before, in which rates have been computed based on Shannon's formula, now rates will be computed considering ideal link adaptation following the link level results from Refs. [5, 37], aiming to a more realistic approach. A total of 15 different Modulation and Coding Schemes (MCSs) are considered and we consider an error free communication. Hence, the maximum rate achieved in a link is approximately 23.31 Mbps. Once in the cellular mode we have two phases with two links in each phase the maximum sum rate achieved is 46.62 Mbps whenever spatial multiplexing is not considered. Instead, when we consider the D2D communication we have the two phases with three links and the maximum sum rate achieved is 69.72 Mbps.

One important parameter to be studied is the adjustment factor δ_R presented in (3.8), which choose if the rate-based mode will be performed. In Fig. 3.21 we illustrate the best values of δ_R for a MIMO 2×4 scheme. As we observe in the figure, the rate-based mode selection scheme assumes a better performance when the variable $\delta_R = -10$. Therefore, the choice of this δ_R parameter is important and its value of -10 will be used from now on.

In Fig. 3.22a we show the CDF of sum rate in SISO case, where 60 % of the cases have sum rate of at least 41.34 Mbps when only cellular mode is enabled. When we apply both practical and the ideal mode selection schemes almost 70 % of all devices

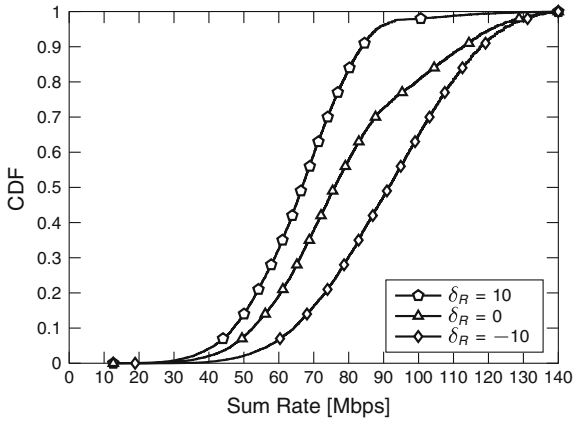

Fig. 3.21 Comparison between three different values of δ_R for the 2×4 case

have sum rate of at least 60.61 Mbps. Moreover, the usage of either rate-based or ideal mode selection can substantially increase the system sum rate.

We show now the CDF of sum rate comparing the rate-based and the ideal mode selection scheme with the simple cellular mode for the ZF filter in two MIMO configurations: 2×2 and 4×4. In Fig. 3.22b, approximately 50 % of all devices have rates of at least 71.4 Mbps considering only the cellular mode. Applying the practical and the ideal mode selection approximately 50 % of all devices have at least 93.32 Mbps. The best results considering the ZF filter are found in Fig. 3.22c because approximately 35 % of all devices have at least 151.7 Mbps considering the mode selection schemes.

Therefore, the proposed mode selection scheme show better performance than pure cellular network in favorable scenarios for D2D communication. Besides that, the proposed scheme shows approximately the same sum rate of the ideal mode selection with perfect channel information. Regarding SISO systems, the mode selection schemes show an improvement in the maximum sum rate in about 50 %.

3.3.2 Resource Block Allocation

Herein we present the performance evaluation for the resource allocation algorithms introduced in Sect. 3.2.3. The simulation parameters are aligned with Table 3.1, but considering that D2D-capable UEs are located inside an hotspot zone placed at cell-edge with radius of 50 m and using MIMO 2×4 configuration.

Figure 3.23 shows the achieved sum rates, where all graphics have three curves:

- The first curve is the CDF of the sum rate achieved when only the cellular mode is enabled;
- The second one is the CDF of the sum rate achieved by employing a mode selection algorithm explained in Sect. 3.2.2; and

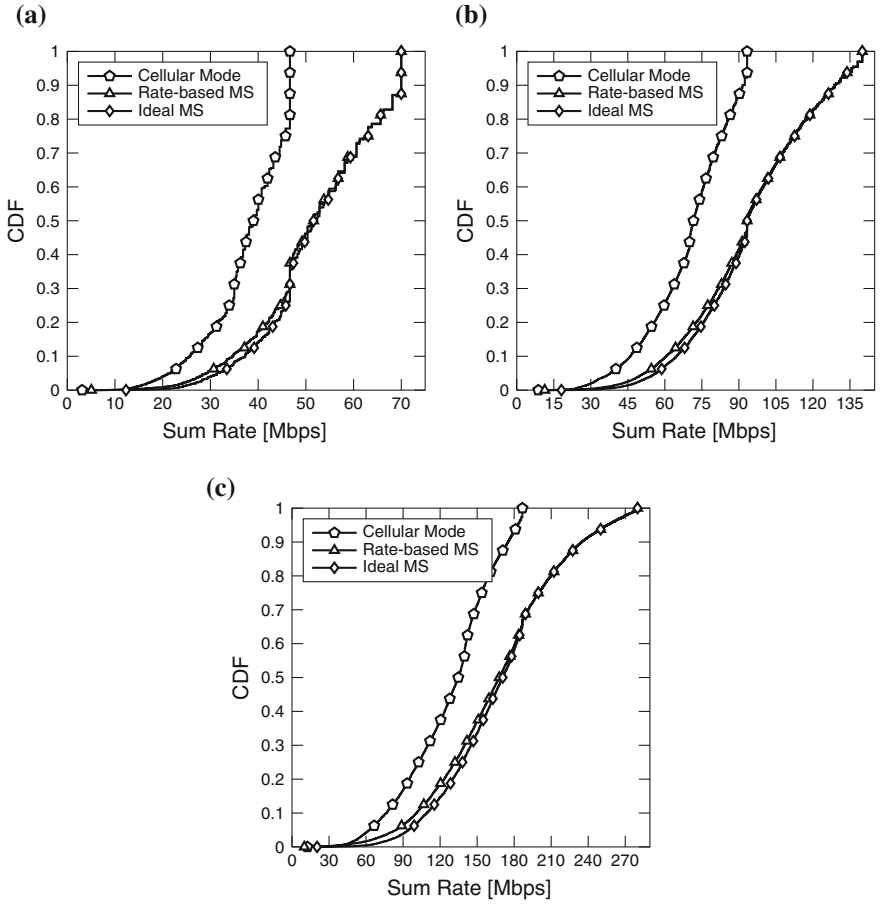

Fig. 3.22 Comparison between mode selection schemes for SISO and MIMO. **a** SISO. **b** MIMO 2×2 with ZF filter. **c** MIMO 4×4 with ZF filter

- The third is the CDF of the sum rate obtained by always choosing the highest rate among cellular and D2D modes, i.e., using ideal mode selection.

Moreover, Fig. 3.23a presents the CDF sum rates when the RR scheduler is used, Fig. 3.23b represents the sum rate achieved when using the RM scheduler with the policy of uplink rate maximization of cellular mode, and Fig. 3.23c uses the same scheduler as the latter but with the policy of uplink rate maximization of D2D mode.

Results show that the adaptive use of D2D communications provide rate gains considering both RR and RM scheduling algorithms. As expected, RM policies provide higher rates than RR and, when comparing different RM policies, we can see that the highest gains are achieved for the maximization of uplink rate of D2D mode.

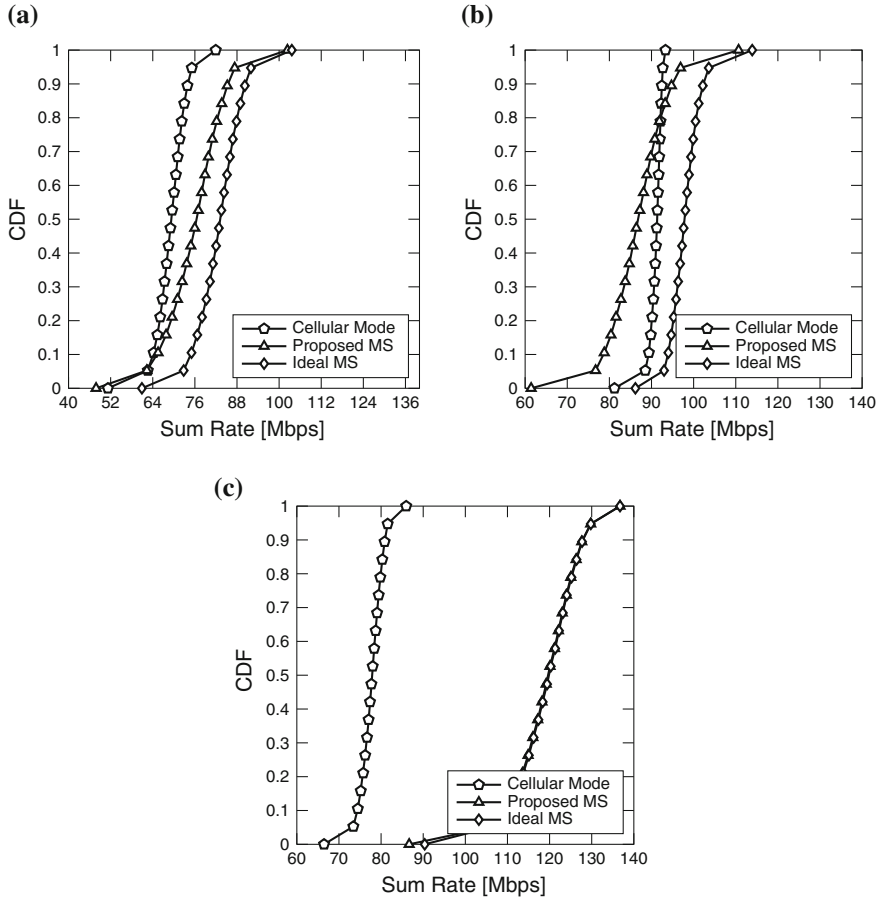

Fig. 3.23 Sum rates in the uplink for different resource block allocation algorithms. **a** Round robin. **b** RM with cellular rate maximization. **c** RM with D2D rate maximization

By exploiting the proximity of D2D-capable UEs, considerable rate gains can be achieved, which for small hotspot radius have a large impact on the overall system performance. If a group that maximizes the rate in cellular mode is chosen, as shown in Fig. 3.23b, the rate achieved in cellular mode is substantially increased if compared to Fig. 3.23a. Even in this case, the rate gains obtained by applying D2D using ideal mode selection are still considerable, although smaller than when considering the maximization of D2D rate policy, as presented in Fig. 3.23c.

Oppositely, we can see in Fig. 3.23b that even in a scenario with favorable conditions for the D2D mode, i.e., $D2D_{Tx}$ close to $D2D_{Rx}$, if we choose the group that maximizes the cellular rate, the proposed mode selection in some cases fails by choosing the D2D mode because there can be a cellular UE near the eNB. A major

Table 3.2 Simulation parameters for power allocation: fixed target SINR

Parameter	Value
Hotspot radius	50 m
Maximum UE_1 to eNB_1 distance	50 m
Channel model	Block-fading ZMCSCG IID
Precoding scheme	SVD
Number of Tx and Rx antennas	2×2, 2×4, and 4×4
Power allocation convergence parameter η	10^{-4}
Target SINR values	0 dB, 2 dB, …, 26 dB

outcome of this analysis is that both resource allocation and mode selection must be jointly tuned in order to ensure good performance.

3.3.3 Power Allocation

In the following paragraphs we evaluate the performance of the EPA algorithm with fixed target SINR values and of the APA algorithm with fixed and variable target SINR values, which have been described in Sect. 3.2.4. Our analyses consider the two-cell uplink scenario of Fig. 3.3 in Sect. 3.2.1.

We are interested on the impact of power allocation algorithms in scenarios where D2D communication within the cellular system offers benefits in terms of system capacity. Therefore, we limit the distance between $D2D_{Tx}$ and $D2D_{Rx}$ and between UE_1 and eNB_1. Moreover, we also consider a low-mobility scenario with a block-fading ZMCSCG IID channel model in which the channel responses remain constant for some tens of TTIs during which the power allocation iterates. Table 3.2 describes the main simulation parameters used herein while the remaining simulation parameter values are those provided in Table 3.1. Regarding the power control algorithms, we consider the EPA and APA algorithms with fixed target SINR values and compare the feasibility of the power allocation and total rate of the system described in Sect. 3.2.1.

Initially, we are interested in comparing the probability of having a feasible power allocation when using EPA and APA. We adopt a Monte Carlo simulation approach with a large number of snapshots in which UE_1, $D2D_{Tx}$ and $D2D_{Rx}$ are randomly positioned within the first cell (respecting the limits established in Table 3.2). The UE_2 has its position fixed at the common border of the two cells of Fig. 3.3 and has a fixed target SINR value of 10 dB. For this configuration, the probability of having a feasible power allocation can be described as the ratio between the number of snapshots in which the power allocation reached the target SINR values for all links and the total number of snapshots. We consider as unfeasible a power allocation in which the algorithms do not converge to a viable solution in less than 50 TTIs.

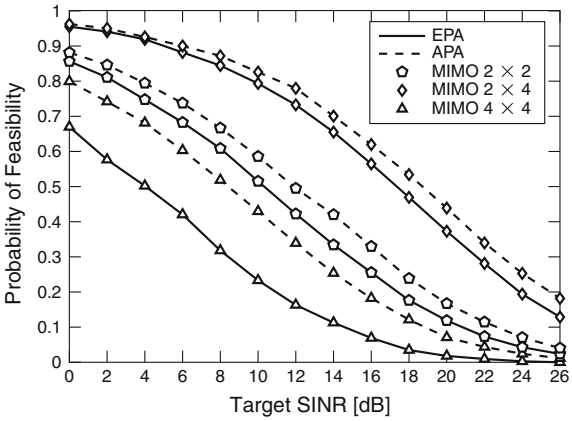

Fig. 3.24 Probability of feasible power allocation as a function of Γ_k in the D2D mode

Figure 3.24 shows the probability of feasibility of the power allocation for the EPA and APA algorithms for different antenna configurations considering D2D communication mode described in Sect. 3.2.2.

As it can be seen in Fig. 3.24, the higher the target SINR value is, the lower the feasibility becomes. From these results, we can also see that for any fixed target SINR value, the APA algorithm increases the feasibility of the power allocation compared to the EPA one. In other words, for a fixed feasibility value, we can see that the APA algorithm is able to attain higher SINR values compared to the EPA algorithm, which will be reflected in better system performance in terms of QoS and/or capacity.

The difference in feasibility values between the two schemes is higher when more antennas are considered. A larger number of the antennas decreases the efficiency of EPA so that for a 4×4 system and a target SINR of 8 dB, its feasibility is around 30 %, while for APA it is around 50 %. The decrease in the feasibility with the number of antennas is related to the higher spatial multiplexing and the higher power sharing among multiple streams. With more antennas, there are more interfering sources (of course with lower power) which make it harder to profit from the spatial filtering ability of the multiple antennas. However, because the same amount of power must be shared among a larger number of streams, the multiplexing gain partially compensates for the reduction in the available power per stream and the more spatially spread interference.

Considering the definitions presented in Sect. 3.2.1, we can calculate the sum rate in each feasible snapshot considering either the cellular or D2D communication mode. By assuming that unfeasible snapshots have sum rate equal to zero and by taking the average of the sum rate values obtained in the feasible snapshots, we can express a modified sum rate as the product between the probability of feasibility of each power allocation scheme and the average sum of the feasible snapshots. This modified sum rate provides some insights on the relative performance of the EPA and APA algorithms in cellular and D2D modes. Figure 3.25 shows this modified

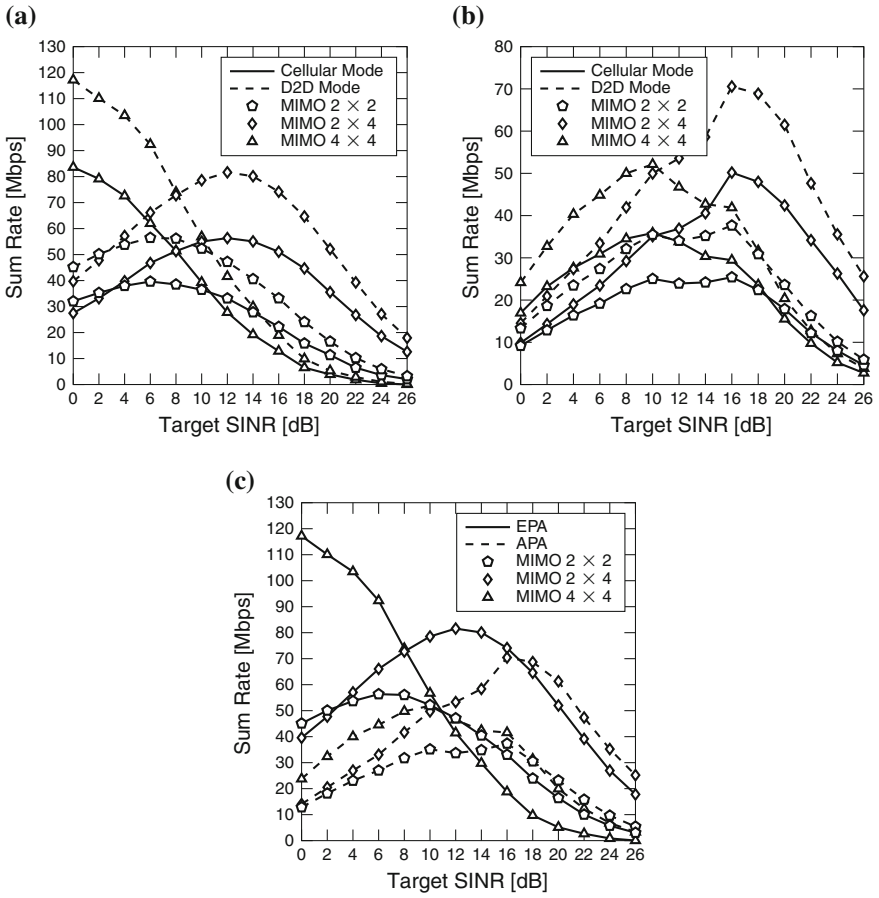

Fig. 3.25 Modified sum rate for EPA and APA algorithms as function of Γ_k. **a** EPA: cellular and D2D modes. **b** APA: cellular and D2D modes. **c** APA versus EPA: D2D mode

sum rate for the EPA and APA algorithms in cellular and D2D modes, as well as compares the performance of both algorithms.

In Figs. 3.25a, b we can see that the performance of D2D communication with power allocation is better than the cellular one for all target SINR values and MIMO schemes. For instance, the 2×4 case with a target SINR of 12 dB in Fig. 3.25a has a relative sum rate gain of approximately 45 % in the D2D mode than in the cellular mode.

As the results in Figs. 3.25a, b shows at low-to-moderate target SINR values, the 4×4 case obtains higher sum rates while the 2×4 scheme has better performance at high target SINR values. This happens because the sum rate of the 4×4 case falls quickly to zero at high SINR values due to low feasibility levels. On the other hand,

Table 3.3 Simulation parameters for power allocation: variable target SINR

Parameter	Value
Number of UEs	100
Number of PRBs	25
Channel model	ZMCSCG IID with 3GPP typical urban micro profile
Scheduling algorithm	RR
% of D2D UEs	50 %
Number of Tx and Rx antennas	1×1, 2×4
Control parameter β	0.3
Maximum Tx power $p_{\max}$	24 dBm
Minimum Tx power $p_{\min}$	-6 dBm
Maximum target SINR $\Gamma_{\max}$	20 dB
Minimum target SINR $\Gamma_{\min}$	-5 dB

a larger receive antenna array reduces the variation of the channel and increases the feasibility at high target SINR.

Figure 3.25c compares the performance of two power allocation algorithms in D2D mode. Therein, we can see that EPA significantly outperforms APA at low-to-moderate target SINR. However, APA has better sum rate at high target SINR values. The high sum rates obtained by EPA are a result from the proximity of the D2D pair and the small distance between UE_1 and eNB_1. Also notice that EPA, when feasible, only achieves "precisely" the target SINR value for the worst stream while the others streams often perceive higher SINR values and consequently achieve higher rates. For the APA algorithm, the target SINR is "precisely" reached for all streams. Hence, when the target SINR increases, the APA gets better due its higher capacity to deal with the infeasibility, a fact that can be observed in the performance curves for 4×4 antenna configuration. For a target SINR equal to 6 dB, APA achieves 44.5 Mbps of sum rate, while EPA achieves 92.3 Mbps.

Regarding convergence, both algorithms have approximately the same performance and converge after 2 to 30 iterations (TTIs). Regarding the total power required to attain a given target SINR value, however, the APA algorithm presents better performance figures than the EPA algorithm and requires less 30 % of power required by latter in the 2×2 and 2×4 cases and less than 12 % in the 4×4 case.

In order to further improve the performance of the APA algorithm, we now consider that a variable target SINR is employed according to the model described in Sect. 3.2.4. Most of the simulation parameters considered in the sequel are the same of Tables 3.1 and 3.3. Differently from the previous configuration, we consider now a multiuser multiresource scenario in which PRBs are allocated according to the RR scheme describe in Sect. 3.2.3 in order to assigning roughly the same number of PRBs to every group of UEs. A total of 100 UEs, of which 50 % are D2D-capable UEs, were randomly distributed in the first cell.

The factor β used for the APA algorithm with variable target SINR has been set to $\beta = 0.3$. One can show that $\beta \leq 1/(1-\rho) = 0.5$ is required for the convergence

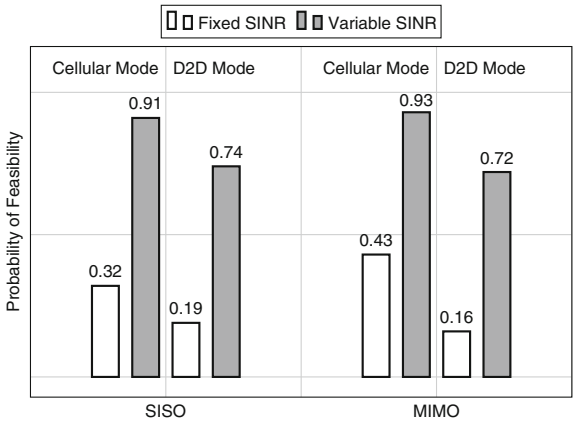

Fig. 3.26 Average probability of feasibility of APA for cellular and D2D modes

of the power control iteration [36, 38]. In general the higher the value of β, the faster the algorithm converges. In fact, for the results presented in the sequel, the APA algorithm converged within less than 10 iterations (TTIs).

Initially, Fig. 3.26 compares the probability of feasibility of the power allocation for cellular and D2D communication modes when 1×1 and 2×4 antenna configurations are considered with the APA using either a fixed or a variable target SINR. Therein, we have set to 15 dB the target SINR value in the fixed target SINR case. From the results, we observe that case with variable target SINR presents a substantially increased feasibility of the power allocation to D2D and cellular communication modes. Since each link/stream aims at trading higher transmit powers to lower target SINR, the available power is used efficiently, power allocation becomes considerably more flexible and, as a consequence, its feasibility is increased.

Looking at Fig. 3.26, we can also see that the percentage of feasible realizations for the cellular mode is higher than that achieved using D2D mode in both 1×1 and 2×4 cases. For example, when APA with variable target SINR is applied for 2×4 case, we have that about 72 % of the snapshots are feasible in the D2D mode while this percentage increases to about 93 % in the cellular mode. The reason for the higher percentage of feasible cases in the cellular mode is associated with the lower interference found in this communication mode. In the D2D mode, the D2D-capable UEs share resources with the cellular UEs, which in turn leads to higher interference and higher occurrence of infeasible cases.

Besides the feasibility of the power allocation, it is important to investigate the overall system capacity when D2D mode is employed. Thus, we evaluated the system performance in terms of sum rate for both communication modes when the APA algorithm is employed in the 1×1 configuration with either a fixed or a variable target SINR. The results are presented in Fig. 3.27, in which the sum rate has been calculated considering only the snapshots with feasible power allocation, otherwise the sum rate has been defined to be zero.

Notice that APA with fixed target SINR, when feasible, only achieves the target SINR value of 15 dB. From the curves, we can see that for fixed SINR, the cellular mode has better performance than the D2D mode. However, when the APA algorithm with variable target SINR is applied, the D2D mode outperforms the cellular mode in nearly 100 % of the cases. The higher sum rates obtained with the D2D mode considering variable target SINR values are mainly an effect of the adjustment of the target SINR as function of the demanded power, which leads to higher feasibility and better exploitation of the benefits of the D2D communication mode discussed in previous sections.

Figure 3.28 presents a similar analysis to the preceding one, but now for the 2×4 configuration. Again, we can see that the sum rate in the cellular mode is always higher than the sum rate obtained with the D2D mode for a fixed target SINR. However, this behavior changes when the APA with variable SINR is applied. In this case, the D2D mode outperforms the cellular mode in a fraction of the cases, thus presenting higher sum rate values.

It is worth to highlight that in the D2D mode there are more interfering sources which makes it harder to profit from spatial filtering ability of multiantenna systems. Moreover, the link between $D2D_{Tx}$ and $D2D_{Rx}$ in the D2D mode is a 2×2 link while the link between the $D2D_{Tx}$ and the eNB_1 considered in the cellular is a 2×4 link. Therefore, this result also shows that the benefits of the D2D communication mode not only strongly depend on the position of the UEs, but also on the capability of the involved UEs and eNBs.

In summary, the previous results reveal that power allocation algorithms with fixed and variable target SINR values are a key RRM functionality to provide improved system performance when a D2D communication mode is employed within cellular networks.

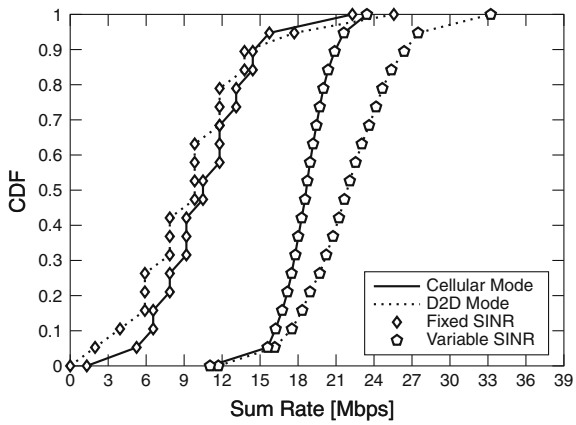

Fig. 3.27 APA sum rate comparison with fixed and variable target SINR for 1×1 configuration

3.3.4 User Grouping

Herein we present the results considering that only one D2D pair is sharing the resources of a cellular UE. We compare the distance-based grouping algorithm with the random UE grouping in the scenarios with and without hotspot described in Sect. 3.2.2. In addition, we will employ MIMO 2 × 2 and 2 × 4 configurations with MMSE spatial filtering.

Figure 3.29 compares the random grouping with the distance-based grouping algorithm described in Sect. 3.2.5 and considering a 2 × 2 antenna configuration. Therein, we show the CDF of sum rate comparing the ideal mode selection scheme with pure cellular mode. In Fig. 3.29a we consider that D2D-capable UEs are uniformly dropped within the cell. In Fig. 3.29b we consider that the D2D-capable UEs are placed inside the hotspot zone.

It can be seen that the distance-based grouping method increases the sum rate of the two communication modes. This sum rate gain is more evident when the D2D UEs are placed inside the hotspot.

Figure 3.30 presents a similar analysis to the preceding one, but now for MIMO 2 × 4 configuration. As expected, the sum rates obtained by this configuration are higher than those obtained by 2 × 2 configuration. Again, we can see the distance-based grouping strategy has better performance than the random grouping strategy for both scenarios, as shown in Figs. 3.30a, b. When the hotspot zone is considered, the sum rate that the system can achieve is significantly increased. Notice that the distance-based grouping method configures groups where sharing resources between D2D-capable and cellular UEs causes low interference.

Now, we will consider that more than one D2D pair can share resources with a cellular UE. The goal is to evaluate the impact of reusing the same resource by multiples D2D pairs on the global system performance. Again, we will consider scenarios with unrestricted UEs positioning and within the hotspot. In this part, we will assume MIMO 2 × 4 configuration with MMSE spatial filtering.

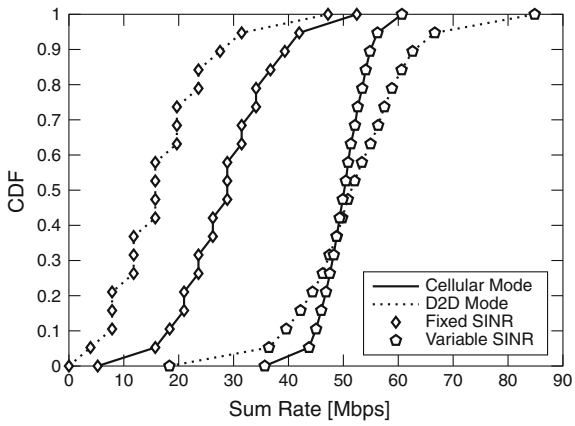

Fig. 3.28 APA sum rate comparison with fixed and variable target SINR for 2 × 4 configuration

Figures 3.31 and 3.32 compares the random grouping with the distance-based grouping when we vary the number of D2D pairs reusing the same resources. Figure 3.31 considers that all users are uniformly distributed in the cell while Fig. 3.32 assumes the existence of an hotspot for D2D-capable users. We utilize the cellular mode as reference system to the different configurations of UEs positioning and D2D pairs.

We can see that the ideal mode selection together with distance-based grouping presents the better sum rate performance for all cases. For two D2D pairs, the sum rate obtained when using a hotspot is significantly higher than that when the distance between the D2D-capable users is not limited. However, this behavior is different when we increase the number of D2D pairs transmitting over the same resources as the cellular UEs. We may note that the gap between the cellular and ideal mode selection when using random grouping or distance-based grouping metric decreases significantly with the increasing number of D2D pairs.

In a scenario with an hotspot, the amount of interference among D2D users transmitting is higher since they are near each other. Therefore, even in a scenario favorable to the D2D mode, i.e., when the distance between the D2D-capable users is limited and they are located at cell-edge, the reuse of resources of a cellular user by three or more D2D users does not show substantial gain compared to the performance achieved in a scenario without hotspot as can see observed in Figs. 3.32b, c and 3.33b, c. Notice that, even in these cases, the rates obtained by applying ideal mode selection using distance-based grouping still provide a slightly gain compared to the mode selection with random grouping and to cellular mode. This is explained by the increase of the D2D rates, which are maximized by the adopted RM policy used here.

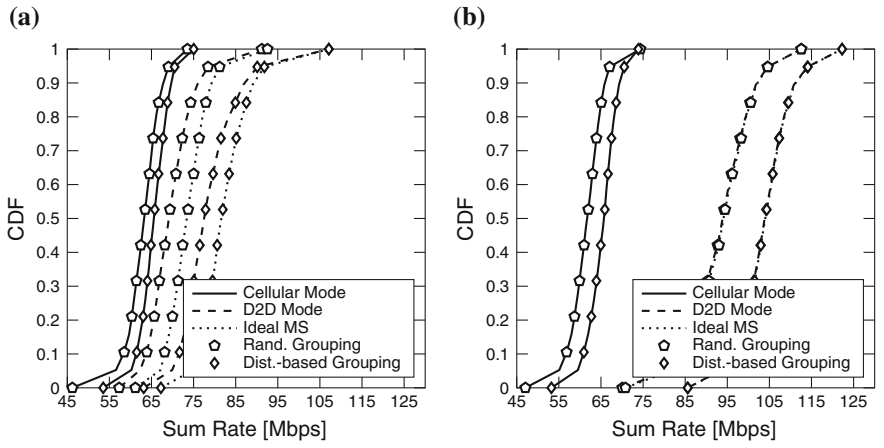

Fig. 3.29 Distance-based algorithm for MIMO 2 × 2 with one D2D pair sharing resources. **a** Unrestricted UE positioning. **b** D2D UE positioning in a hotspot

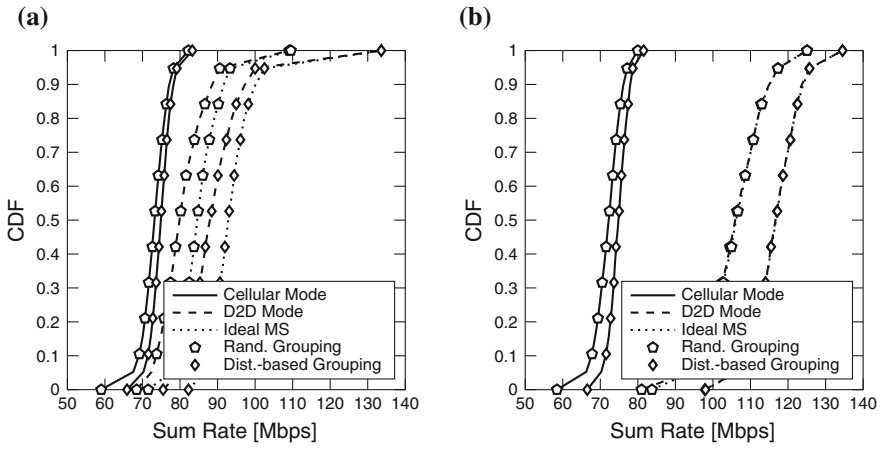

Fig. 3.30 Distance-based algorithm for MIMO 2×4 with one D2D pair sharing resources. **a** Unrestricted UE positioning. **b** D2D UE positioning in a hotspot

Figure 3.33 compares the sum rate when the three grouping strategies are employed. We vary the number of D2D pairs number when the D2D users are placed in a hotspot. We employ three Single-Input Multiple-Output (SIMO) configurations: 1×3, 1×4, and 1×5 with two, three and four D2D pairs, respectively. From the figures, we can see that the successive allocation-based grouping, described in Sect. 3.2.5, outperforms the distance-based and random grouping strategies. For example, in the Fig. 3.33c, 50 % of the users have sum rate of 50 Mbps for the former algorithm, while the same amount of the users have around 36 and 38 Mbps of sum rate when the random grouping and distance-based grouping are considered, respectively.

The higher sum rate obtained by the successive allocation-based algorithm is mainly an effect of the spatial subchannel allocation method, in which no interference is generated to any of the subchannels that form a certain group. Once the groups are built via this algorithm, the eNB uses a ZF filter to communicate to cellular UE and neutralize the interference originated by the transmitting D2D UE established in the same group. Simultaneously, the D2D pairs use MRC filters to communicate to each other. The performance gain achieved by successive allocation-based grouping method of spatial channels can be a solution to explore the reuse gain of the D2D communication in situations where multiple D2D pairs are reusing the same resources with a cellular UE.

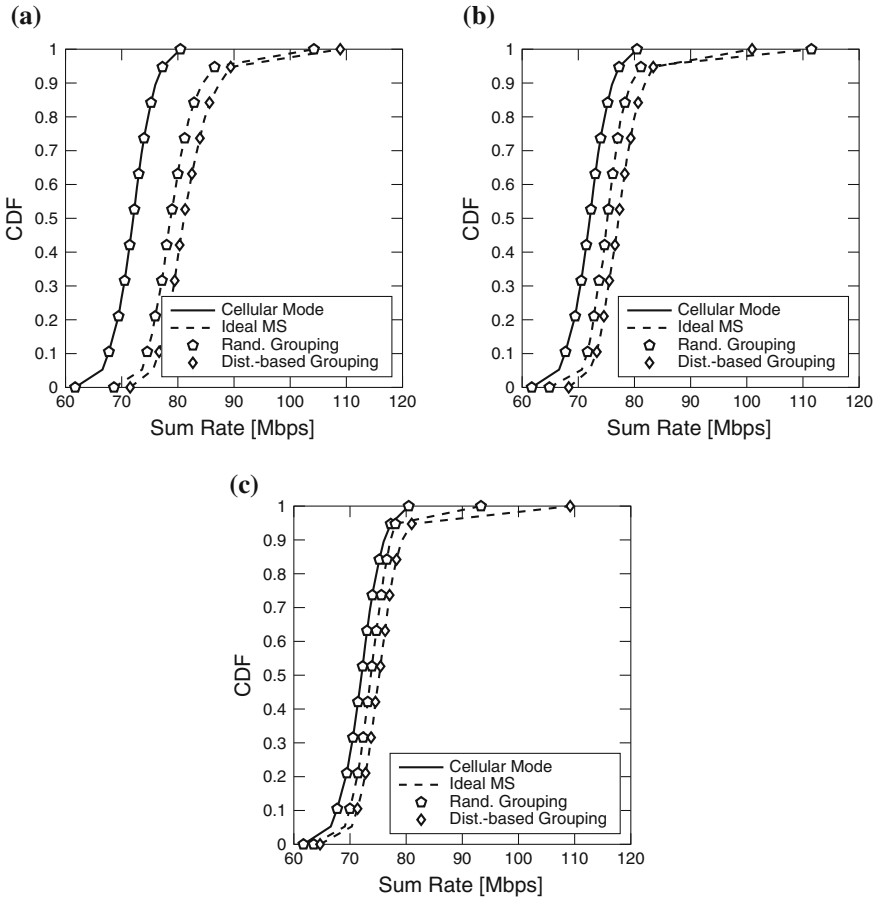

Fig. 3.31 Comparison between grouping strategies for number of D2D pairs varying and unrestricted positioning. **a** Two D2D pairs. **b** Three D2D pairs. **c** Four D2D pairs

3.4 Conclusions

In this chapter we introduced the concepts for D2D communications, trying to give a global view from the neighbor discovery until the link establishment. The chapter started with the presentation of the related principals and a literature review for D2D communication mechanisms. Then the attentions were concentrated in the RRA techniques and their possible performance enhancements.

Regarding mode selection, we have made a study on the impact of the distance between $D2D_{Tx}$ and eNB_1 and the distance between UE_1 and $D2D_{Rx}$ on the performance of D2D and cellular communication modes. Both results have shown that the percentage of success of the D2D mode is almost zero when the distances between

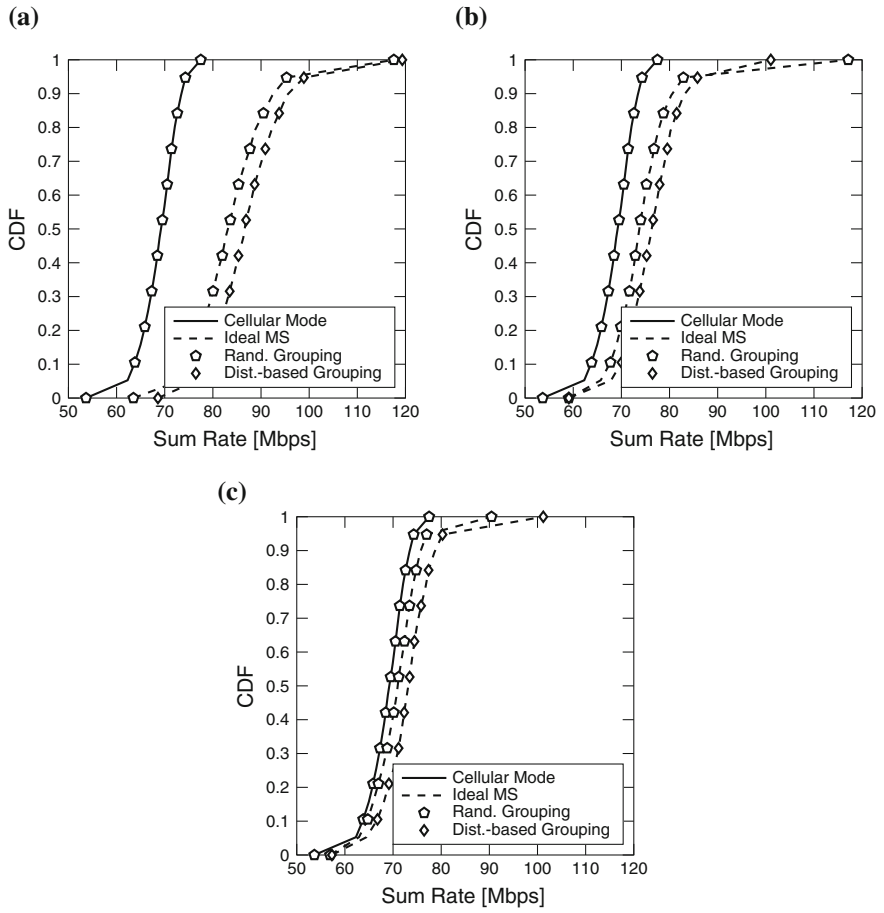

Fig. 3.32 Comparison between grouping strategies for number of D2D pairs varying and positioning in a hotspot. **a** Two D2D pairs. **b** Three D2D pairs. **c** Four D2D pairs

these pairs of interfering nodes are close to zero, thus illustrating the D2D communication should not be applied all the time, but only in some favorable conditions.

In the sequel, we have studied how a restriction in the UE_1 positioning—the near eNB and near cell-edge regions—and the distance between $D2D_{Tx}$ and $D2D_{Rx}$ could improve the sum rate of the system. We have shown that when UE_1 is in the near eNB region, the rates are greater than when it is in the near cell-edge region. Moreover, we have also shown that when we restrict the $d_{\text{Tx-Rx}}$ between the D2D UE, the rates achieved by the D2D mode are greater than those of the cellular mode even in the near cell-edge region; where without the restriction, the rates were always lower than the cellular mode ones.

We have also proposed one mode selection algorithm: the rate-based mode selection. The proposed scheme has shown better performance than pure cellular network

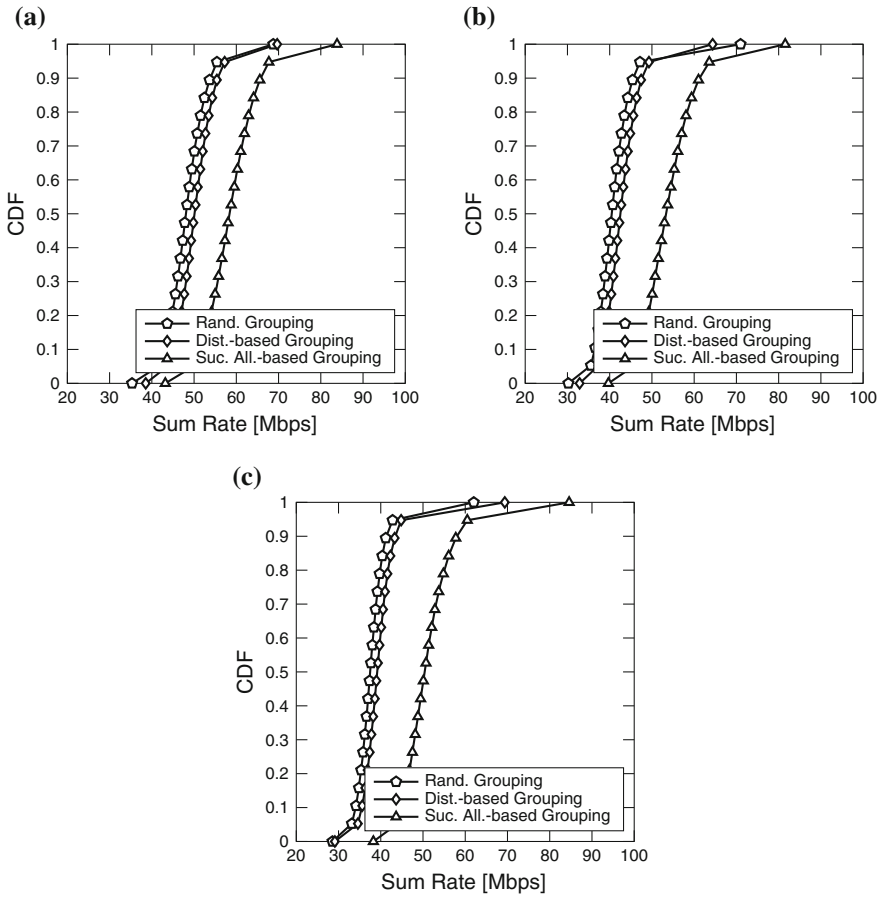

Fig. 3.33 Comparison between the grouping strategies for D2D pairs number and MIMO configuration varying. **a** Two D2D pairs and 1×3 scheme. **b** Three D2D pairs and 1×4 scheme. **c** Four D2D pairs and 1×5 scheme

in scenarios favorable for D2D communication. Besides that, it has shown approximately the same sum rate of the ideal mode selection with perfect CSI. We also have considered multiple antennas at the transmit and receiver sides. Then, the mode selection schemes associated to multiple antennas exhibit an improvement in the maximum sum rate of about 50 % in SISO and SIMO cases. Considering MIMO configurations, the ZF precoder associated with mode selection has presented expressive sum rate gains compared to the previous scenarios. These gains can be converted in different ways by the operators, e.g., in more users sharing the free resources or even higher data rates for the existing users.

We have also studied the schedulers RR and RM. Results show that the adaptive use of D2D communications provides rate gains considering both scheduling algorithms;

but the highest gains are achieved with RM for the maximization of uplink rate of D2D mode.

Generally, by exploiting the proximity of D2D-capable UEs, considerable rate gains can be achieved, which for small hotspot radius have a large impact on the overall system performance. Nevertheless, it is important to take in mind that even in a scenario with favorable conditions for the D2D mode, if we choose the group that maximizes the cellular rate, the proposed mode selection in some cases fails by choosing the D2D mode. A major outcome of this analysis is that both scheduling and mode selection must be jointly tuned in order to ensure good performance.

Considering the power allocation, we have studied different power allocation algorithms with fixed or variable target SINR and in single or multiple antenna scenarios. In general, we have shown that adaptive power allocation can improve the benefits of a D2D mode within a cellular system. In particular, we have shown that when using an adaptive power allocation with variable target SINR, we could improve considerably the feasibility of power allocations, which represents better provision of QoS to the UEs in the system, as well as enhanced system capacity in terms of sum rate. Besides showing that power allocation can improve the performance of D2D communications within cellular systems, we have also illustrated that these performance gains depend on scenario and antenna configurations, as it has been the case when studying other RRA techniques within this chapter.

The user grouping and its impact on the cellular network have also been studied, where we developed two mixed cellular and D2D UEs strategies that have dealt with the distance between the D2D and the serving eNB and with allocation of spatial subchannels. In the first strategy, we proposed an grouping algorithm based on link distances from transmitting UEs to eNB. In the second strategy, we extended a grouping algorithm based on successive allocation of spatial channels to a mixed cellular and D2D environment. The results demonstrate that for both methods the sum rate of the cellular network with D2D communication mode outperforms that of the pure cellular network considerably. Moreover, the successive allocation-based grouping algorithm has presented better performance than the distance-based one.

In summary, the results and relative performance comparisons presented in this chapter have richly illustrated the potential gains of D2D communications underlaying a cellular network. Nevertheless, it still exists a considerable room for further research on D2D communications, where we can mention:

- Further investigations of RRM techniques in multiuser and multicell scenarios.
- Study of band selection (downlink or uplink) algorithms to mitigate the interference generated due to D2D communication inside/outside of its serving cell.
- Study of neighbor discovery methods capable of working in a multicell network while being (or not) network-assisted.
- Selective usage of D2D communications, e.g., not enabling it in all PRBs but only when the impact in cellular communications is minimum.
- Proposal of algorithms that take jointly into account mode selection, power control and resource allocation.

- Proposal of techniques that improve the network capacity, e.g., by allowing more than one D2D pair to share the same resource.
- Proposal of grouping algorithms that consider the distance between the D2D pair for the assignment of the spatial subchannels as well as the distance from them to the eNB, among others.

References

1. 3GPP: Evolved universal terrestrial radio access (E-UTRA); base station (BS) radio transmission and reception. TS 36.104, 3rd Generation Partnership Project (3GPP) (2009). http://www.3gpp.org/ftp/Specs/html-info/36104.htm. V9.0.0
2. 3GPP: Evolved universal terrestrial radio access (E-UTRA); further advancements for E-UTRA physical layer aspects. TR 36.814, 3rd Generation Partnership Project (3GPP) (2010). http://www.3gpp.org/ftp/Specs/html-info/36814.htm. V9.0.0
3. 3GPP: Evolved Universal Terrestrial Radio Access (E-UTRA); Multiplexing and channel coding. TS 36.212, 3rd Generation Partnership Project (3GPP) (2009). http://www.3gpp.org/ftp/Specs/html-info/36212.htm. V9.0.0
4. 3GPP: Evolved Universal Terrestrial Radio Access (E-UTRA); Physical Channels and Modulation. TS 36.211, 3rd Generation Partnership Project (3GPP) (2009). http://www.3gpp.org/ftp/Specs/html-info/36211.htm. V9.0.0
5. 3GPP: Evolved universal terrestrial radio access (E-UTRA); physical layer procedures. TS 36.213, 3rd Generation Partnership Project (3GPP) (2009). http://www.3gpp.org/ftp/Specs/html-info/36213.htm. V9.0.1
6. 3GPP: Evolved universal terrestrial radio access (E-UTRA); user equipment (UE) radio transmission and reception. TS 36.101, 3rd Generation Partnership Project (3GPP) (2009). http://www.3gpp.org/ftp/Specs/html-info/36101.htm. V9.0.0
7. 3GPP: Physical layer aspects for evolved universal terrestrial radio access (UTRA). TR 25.814, 3rd Generation Partnership Project (3GPP) (2006). http://www.3gpp.org/ftp/Specs/html-info/25814.htm. V7.1.0
8. 3GPP: Spatial channel model for multiple input multiple output (MIMO) simulations. TR 25.996, 3rd Generation Partnership Project (3GPP) (2012). http://www.3gpp.org/ftp/Specs/html-info/25996.htm. V11.0.0
9. An, X., Hekmat, R.: Self-adaptive neighbor discovery in ad hoc networks with directional antennas. In: 16th IST Mobile and Wireless Communications Summit, 2007, pp. 1–5 (2007)
10. Angelosante, D., Biglieri, E., Lops, M.: A simple algorithm for neighbor discovery in wireless networks. In: IEEE International Conference on Acoustics, Speech and Signal Processing, 2007. ICASSP 2007, vol. 3, pp. III-169-III-172 (2007)
11. Angelosante, D., Biglieri, E., Lops, M.: Neighbor discovery in wireless networks: a multiuser-detection approach. Phys. Commun. **3**(1), 28–36 (2010)
12. Belleschi, M., Fodor, G., Abrardo, A.: Performance analysis of a distributed resource allocation scheme for D2D communications. In: IEEE GLOBECOM Workshops (GC Wkshps), 2011, pp. 358–362 (2011). doi:10.1109/GLOCOMW.2011.6162471
13. Caire, G., Shitz, S.S.: On the achievable throughput of a multiantenna Gaussian broadcast channel. IEEE Trans Inf Theory **49**(7), 1691–1706 (2003). doi:10.1109/TIT.2003.813523
14. Camarillo, G.: Peer-to-peer (P2P) architecture: Definition, taxonomies, examples, and applicability. RFC 5694, RFC Editor (2009)
15. Cavalcanti, F.R.P., Andersson, S. (eds.): Optimizing Wireless Communication Systems. Springer, New York (2009)
16. Chen, R., Andrews, J.G., Heath, R.W., Ghosh, A.: Uplink power control in multi-cell spatial multiplexing wireless systems. IEEE Trans Wireless Commun **67**, 2700–2711 (2007). doi:10.1109/TWC.2007.051007

17. Cover, T.M., Thomas, J.A.: Elements of Information Theory, 2nd edn. Wiley Series in Telecommunications and Signal Processing. Wiley-Interscience, New York (2006)
18. da S. Rêgo, M.G., Maciel, T.F., de Holanda Madeira Barros, H., Cavalcanti, F.R.P., Fodor, G.: Performance analysis of power control for device-to-device communication in cellular MIMO systems. In: IEEE International Symposium on Wireless Communication Systems (2012)
19. Doppler, K., Manssour, J., Osseiran, A., Xiao, M.: Innovative concepts in peer-to-peer and network coding. Deliverable 1.3, WINNER + (2009)
20. Doppler, K., Ribeiro, C.B., Kneckt, J.: Advances in D2D communications: energy efficient service and device discovery radio. In: 2011 2nd International Conference on Wireless Communication, Vehicular Technology, Information Theory and Aerospace and Electronic Systems Technology (Wireless VITAE), pp. 1–6 (2011)
21. Doppler, K., Yu, C.H., Ribeiro, C.B., Jänis, P.: Mode selection for device-to-device communication underlaying an LTE-advanced network. In: IEEE, Wireless Communications and Networking Conference, pp. 1–6 (2010)
22. Doppler, K., Rinne, M., Wijting, C., Ribeiro, C.B., Hugl, K.: Device-to-device communication as an underlay to LTE-advanced. IEEE Commun. Mag. **47**(12), 42–49 (2009)
23. ETSI: Terrestrial trunked radio (TETRA); voice plus data (V+D); part 2:air interface (AI). ETSI TS 100 392–2, European Telecommunications Standards Institute (ETSI) (2011) V3.5.1.
24. Felemban, E., Murawski, R., Ekici, E., Park, S., Lee, K., Park, J., Hameed, Z.: SAND: sectored-antenna neighbor discovery protocol for wireless networks. In: 2010 7th Annual IEEE Communications Society Conference on Sensor, Mesh and Ad Hoc Communications and Networks (SECON), pp. 1–9 (2010)
25. Fodor, G., Dahlman, E., Mildh, G., Parkvall, S., Reider, N., Miklós, G., Turányi, Z.: Design aspects of network assisted device-to-device communications. IEEE Commun. Mag. **50**(3), 170–176 (2012)
26. Foschini, G.J., Miljanic, Z.: A simple distributed autonomous power control algorithm and its convergence. IEEE Trans Veh Technol **42**(4), 641–645 (1993). doi:10.1109/25.260747
27. Gossain, H., Cordeiro, C., Cavalcanti, D., Agrawal, D.P.: The deafness problems and solutions in wireless ad hoc networks using directional antennas. In: IEEE Global Telecommunications Conference Workshops, 2004. GlobeCom Workshops 2004, pp. 108–113 (2004)
28. Gupta, S., Yates, R.D., Rose, C.: Soft dropping power control—a power control backoff strategy. In: IEEE International Conference on Personal, Wireless Communications, pp. 210–214 (1997)
29. Hakola, S., Chen, T., Lehtomaki, J., Koskela, T.: Device-to-device (D2D) communication in cellular network—performance analysis of optimum and practical communication mode selection. In: IEEE, Wireless Communications and Networking Conference, pp. 1–6 (2010)
30. Jang, J., Lee, K.B.: Transmit power adaptation for multiuser OFDM systems. IEEE J. Sel. Areas Commun. **21**(2), 171–178 (2003)
31. Jänis, P., Koivunen, V., Ribeiro, C.B., Doppler, K., Hugl, K.: Interference-avoiding MIMO schemes for device-to-device radio underlaying cellular networks. In: 2009 IEEE 20th International Symposium on Personal, Indoor and Mobile Radio, Communications (PIMRC'09), pp. 2385–2389 (2009)
32. Jänis, P., Koivunen, V., Ribeiro, C., Korhonen, J., Doppler, K., Hugl, K.: Interference-aware resource allocation for device-to-device radio underlaying cellular networks. In: Vehicular Technology Conference, 2009. VTC Spring 2009. IEEE 69th, pp. 1–5 (2009)
33. Jänis, P., Yu, C.H., Doppler, K., Ribeiro, C., Wijting, C., Hugl, K., Tirkkonen, O., Koivunen, V.: Device-to-device communication underlaying cellular communications systems. Int. J. Commun. Network Syst. Sci. **2**(3), 169–178 (2009)
34. Jung, M., Hwang, K., Choi, S.: Joint mode selection and power allocation scheme for power-efficient device-to-device (D2D) communication. In: IEEE Vehicular Technology Conference (2012)
35. Lin, D.D., Lim, T.J.: Subspace-based active user identification for a collision-free slotted ad hoc network. IEEE Trans. Commun. **52**(4), 612–621 (2004)
36. Maciel, T.F., Klein, A.: On the performance of SDMA with soft dropping and SINR balancing power control in the downlink of multi-user MIMO systems. In: ITG Workshop on Smart Antennas (2007)

37. Mehlführer, C., Wrulich, M., Ikuno, J.C., Bosanska, D., Rupp, M.: Simulating the long term evolution physical layer. In: Proceedings of the 17th European Signal Processing Conference (EUSIPCO 2009). Glasgow, Scotland. http://publik.tuwien.ac.at/files/PubDat_175708.pdf (2009)
38. Papandriopoulos, J., Evans, J., Dey, S.: Distributed power control for cellular MIMO systems with temporal and spatial filtering. In: Australian Communications Theory, Workshop, pp. 164–175 (2004)
39. Paulraj, A., Nabar, R., Gore, D.: Introduction to Space-Time Wireless Communications, 1st edn. Cambridge University Press, Cambridge (2003)
40. Roberts, L.G.: ALOHA packet system with and without slots and capture. Comput. Commun. Rev. **5**(2), 28–42 (1975)
41. Schubert, M., Boche, H.: Solution of the multiuser downlink beamforming problem with individual SINR constraints. IEEE Trans. Veh. Technol. **53**(1), 18–28 (2004)
42. Subramanian, A.P., Das, S.R.: Addressing deafness and hidden terminal problem in directional antenna based wireless multi-hop networks. In: 2nd International Conference on Communication System Software and Middleware and Workshops. COMSWARE 2007, (2007)
43. Tejera, P., Utschick, W., Bauch, G., Nossek, J.A.: Subchannel allocation in multiuser multiple-input multiple-output systems. IEEE Trans. Inf. Theory **52**(10), 4721–4733 (2006). doi:10.1109/TIT.2006.881751
44. Trees, H.L.V.: Optimum Array Processing, 1st edn. Wiley-Interscience, New York (2002)
45. Vasudevan, S., Kurose, J., Towsley, D.: On neighbor discovery in wireless networks with directional antennas. In: Proceedings IEEE INFOCOM 2005. 24th Annual Joint Conference of the IEEE Computer and Communications Societies, vol. 4, pp. 2502–2512 (2005)
46. Vasudevan, S., Towsley, D., Goeckel, D., Khalili, R.: Neighbor discovery in wireless networks and the coupon collector's problem. In: Proceedings of the Annual International Conference on Mobile Computing and Networking. MobiCom'09, pp. 181–192 (2009)
47. Wang, B., Chen, L., Chen, X., Zhang, X., Yan, D.: Resource allocation optimization for device-to-device communication underlaying cellular networks. In: Vehicular Technology Conference (VTC Spring), 2011 IEEE 73rd, pp. 1–6 (2011)
48. Wang, C.X., Hong, X., Ge, X., Cheng, X., Zhang, G., Thompson, J.: Cooperative MIMO channel models: a survey. IEEE Commun. Mag. **48**(2), 80–87 (2010)
49. Xing, H., Hakola, S.: The investigation of power control schemes for a device-to-device communication integrated into OFDMA cellular system. In: IEEE 21st International Symposium on Personal Indoor and Mobile Radio Communications (PIMRC), pp. 1775–1780 (2010). doi:10.1109/PIMRC.2010.5671643
50. Yates, R.D.: A framework for uplink power control in cellular radio systems. IEEE J. Sel. Areas Commun. **13**(7), 1341–1347 (1995). doi:10.1109/49.414651
51. You, L., Yuan, Z., Yang, P., Chen, G.: ALOHA-like neighbor discovery in low-duty-cycle wireless sensor networks. In: 2011 IEEE Wireless Communications and Networking Conference (WCNC), vol. 4, pp. 749–754 (2011)
52. Yu, C., Tirkkonen, O., Doppler, K., Ribeiro, C.: On the performance of device-to-device underlay communication with simple power control. In: Vehicular Technology Conference, 2009. VTC Spring 2009. IEEE 69th, pp. 1–5 (2009). doi:10.1109/VETECS.2009.5073734
53. Yu, C.H., Tirkkonen, O., Doppler, K., Ribeiro, C.: Power optimization of device-to-device communication underlaying cellular communication. In: IEEE International Conference on Communications (ICC), pp. 1–5 (2009). doi:10.1109/ICC.2009.5199353
54. Zhang, L., Guo, D.: Neighbor discovery in wireless networks using compressed sensing with Reed-Muller codes. In: 2011 International Symposium of Modeling and Optimization in Mobile, Ad Hoc, and, Wireless Networks, pp. 154–160 (2011)
55. Zhang, Z., Li, B.: Neighbor discovery in mobile ad hoc self-configuring networks with directional antennas: algorithms and comparisons. IEEE Trans. Wireless Commun. **7**(5), 1540–1549 (2008)
56. Zulhasnine, M., Huang, C., Srinivasan, A.: Efficient resource allocation for device-to-device communication underlaying LTE network. In: Wireless and Mobile Computing, Networking and Communications (WiMob), 2010 IEEE 6th International Conference, pp. 368–375 (2010)